Heterometallic Effects in Trinuclear Complexes Supported by *para*-terphenyl Diphosphine Ligands

Kyle Horak, Sibo Lin, Jonathan Rittle, Theodor Agapie*

*To whom correspondence should be addressed. E-mail: agapie@caltech.edu.
Department of Chemistry and Chemical Engineering, California Institute of Technology, 1200 E. California Blvd. MC 127-72, Pasadena, CA, USA.

Supporting Online Material

Contents

Experimental Section

General Considerations

All air- and/or water-sensitive compounds were manipulated using standard vacuum or Schlenk line techniques or in an inert atmosphere glove box. The solvents for air- and moisture-sensitive reactions were dried over sodium benzophenone ketyl, calcium hydride, or by the method of Grubbs.[1] All NMR solvents were purchased from Cambridge Isotopes Laboratories, Inc. and dried over sodium benzophenone ketyl or calcium hydride. Unless mentioned otherwise, reagents were used as received from commercial suppliers without further purification. Bis(1,5-cyclooctadiene)nickel(0), nickel(II) dichloride dimethoxyethane adduct, tetrakis(acetonitrile)palladium(II) tetrafluroborate, cobaltocene, and tris-(dibenzylideneacetone)dipalladium(0) were ordered from Strem Chemicals, Inc. 2-bromophenylboronic acid was purchased from Ark Pharm, Inc. Chlorodiisopropylphosphine was purchased from Sigma Aldrich. Iodine monochloride was purchased from Alfa Aesar. 1,4-dimethoxy-2,5-diiodobenzene,[2] 1,4-bis(2-diisopropylphosphinophenyl)benzene,[3] compound **6**,[3] $[Pd(MeCN)_3]_2[BF_4]_2$,[4] $Na[Co(CO)_4]$,[5] and $Na_2[Fe(CO)_4]$[6] were synthesized according to literature procedures. All ^1H, ^{13}C, and ^{31}P spectra were recorded on Varian Mercury 300 MHz, or Varian INOVA-500 or 600 MHz spectrometers at room temperature. Chemical shifts for ^1H and ^{13}C NMR data are reported relative to residual solvent peaks and are ^{13}C and ^1H decoupled respectively unless otherwise noted.[7] ^{31}P NMR chemical shifts are reported with respect to the deuterated solvent used to lock the instrument and are ^1H decoupled unless otherwise noted. IR spectra were obtained as solution samples using a CaF_2 window cell on a Thermo Scientific Nicolet 6700 FT-IR spectrometer. Elemental analyses were performed by Robertson Microlit Laboratories, Ledgewood, NJ.

Synthesis of 1,4-bis(2-bromophenyl)-2,5-(dimethoxy)benzene (A)

The Suzuki coupling to produce the terphenyl product was run as a modification of literature procedure.[3] A Schlenk tube fitted with a Teflon stopper was charged with 1,4-dimethoxy-2,5-diiodobenzene (5.00 g, 12.82 mmol, 1 equiv.), 2-bromo-phenylboronic acid (5.41 g, 26.9 mmol, 2.1 equiv.), and K_2CO_3 (10.63 g, 76.9 mmol, 6 equiv.). Toluene (270 mL), ethanol (65 mL), and water (65 mL) were then transferred to the Schlenk tube along with a magnetic stirbar. The mixture was degassed by two freeze pump thaw cycles and then put under positive nitrogen pressure. Under a strong counterflow of nitrogen, $Pd(PPh_3)_4$ (741 mg, 0.64 mmol, 0.05 equiv.) was added and the solution became a pale yellow color. The reaction mixture was then heated to 65 °C and stirred for 16-24 hrs while monitoring the reaction by GC-MS. The volatiles were then removed on a rotovap and the residue triturated with water, then methanol, and finally dichloromethane to yield the product as an off-white powder. Yield: 4.22 g (67 %). ^1H NMR (500 MHz, $CDCl_3$) δ 7.42-7.36 (unresolved m, 4H, aryl-*H*), 7.23 (m, 2H, aryl-*H*), 6.82 (s, 2H, central aryl-*H*), 3.74 (s, 6H, OC*H_3*). ^{13}C NMR (126 MHz, $CDCl_3$) δ 150.20 (s), 129.61 (s), 132.64 (s), 131.68 (s), 130.35 (s), 128.82 (s), 127.04 (s), 124.13 (s), 114.45 (s), 56.39 (s). GC-MS (m/z): Calcd, 447.95 (M$^+$), Found: 448.1 (M$^+$). FAB-MS (m/z): Calcd, 447.9496 (M$^+$), Found: 447.9486 (M$^+$).

Synthesis of 1,4-bis(2-(diisopropylphophino)phenyl)-2,5-(dimethoxy)benzene (4)

Phosphination run as a modification of literature procedures.[3] A Schlenk tube fitted with a screw-in Telfon stopper was charged with 1,4-bis(2-bromophenyl)-2,5-dimethoxybenzene (1.5 g, 3.34 mmol, 1 equiv.) and a magnetic stirbar. Tetrahydrofuran (150 mL) was then to the Schlenk tube. The reaction was cooled to -78 ºC and *tert*-butyllithium (1.7 M pentane solution, 8 mL, 13.7 mmol, 4.1 equiv.) was added while stirring to generate a pale yellow solution. The reaction mixture was allowed to warm to room temperature and then stirred for an additional hour. During this time the solution became a cloudy suspension. Chlorodiisopropyl phosphine (1.12 mL, 7.02 mmol, 2.1 equiv.) was then added to the reaction via syringe. The solution immediately became a homogenous pale yellow solution which was allowed to stir for 16 hours. The volatiles were then removed under reduced pressure on the Schlenk line. The yellowish residue was then suspended in *ca.* 100 mL of toluene and filtered through a Celite pad. The filtrate was then dried under reduced pressure. This residue was then triturated with acetonitrile (*ca.* 20 mL) which removed colored impurities to leave the product as a white powder. Yield: 0.6 g (34 %). ^{1}H NMR spectra of product is broad at room temperature due to hindered rotation around aryl–aryl bonds. This is corroborated by ^{31}P NMR where two distinct peaks are observed at room temperature. ^{1}H NMR (300 MHz, C_6D_6) δ 7.49 (m, 2H, aryl-*H*), 7.43 (m, 2H, aryl-*H*), 7.19 (m, 4H, aryl-*H*), 6.83 (s, 2H, central aryl-*H*), 3.43 (s, 6H, OC*H*$_3$), 2.05 (m, 2H, C*H*), 1.87 (m, 2H, C*H*), 1.06 (m, 24H, C*H*$_3$). ^{31}P{^{1}H} NMR (121 MHz, C_6D_6) δ -1.18 (s), -2.67 (s). This is due to the formation of two different atropisomers at room temperature due to hindered rotation around the aryl-aryl bonds. A single ^{31}P resonance is observed at -0.2 ppm at 70 ºC. ^{13}C{^{1}H} NMR (126 MHz, C_6D_6) δ 149.98 (s), 147.34 (d, J_{PC} = 30.5 Hz), 136.26 (d, J_{PC} = 22.0 Hz), 131.97 (s), 130.90 (s), 130.65 (s), 128.12 (s), 126.33 (s), 115.02 (s), 54.93 (s), 25.42 (broad s), 24.03 (broad s), 23.38 (broad s), 20.35 (broad s), 19.89 (broad s), 19.12 (broad s). GC-MS (m/z): Calcd: 522.28 (M$^+$), Found: 521.2761. FAB-MS (m/z): Calcd: 521.2738 (M$^+$), Found: 521.2761 (M$^+$).

Synthesis of Complex 2

Compound **1** was generated *in situ* from the reaction of 1,4-bis(2-diisopropylphosphinophenyl)benzene (100 mg, 0.216 mmol, 1 equiv.) with [Pd(MeCN)$_3$]$_2$[BF$_4$]$_2$ (MeCN = acetonitrile) (136.8 mg, 0.216 mmol, 1 equiv.). This was accomplished by charging a 20 mL scintillation vial with the 1,4-bis(2-diisopropylphosphinophenyl)benzene and a magnetic stirbar before adding the [Pd(MeCN)$_3$]$_2$[BF$_4$]$_2$ as a solution in acetonitrile (*ca.* 5 mL) and allowing the mixture to stir over 1 hr at room temperature. During this time the solution became a homogeneous red. Formation of **1** could be confirmed by ^{31}P NMR of reaction mixture. Na$_2$[Fe(CO)$_4$] was added as a partially solubilized suspension in tetrahydrofuran (*ca.* 2 mL) at room temperature. The solution immediately became a darker red and the reaction was allowed to stir for 1 hr. Volatiles were then removed under reduced pressure. The residue was suspended in acetonitrile and filtered onto a Celite pad. The solid was washed with additional acetonitrile until washes became colorless. The remaining material was dissolved in tetrahydrofuran filtered through the Celite pad. Removal of volatiles yielded

the product as a red solid. Yield: 80 mg (44 %). Single crystals suitable for X-ray diffraction studies were grown from the vapor diffusion of hexanes into a concentrated tetrahydrofuran:benzene (1:1) solution at room temperature. ^{1}H NMR (300 MHz, C$_6$D$_6$) δ 7.18 (s, 2H, aryl-H), δ 7.11-6.98 (m, 6H, aryl-H), δ 5.92 (s, 4H, central aryl-H), δ 2.26 (m, 4H, CH), δ 1.25 (dd, J$_{PH}$ = 18.1, J$_{HH}$ = 7.0 Hz, 12H, CH_3), δ 0.89 (dd, J$_{PH}$ = 8.5, J$_{HH}$ = 7.2 Hz, 12H, CH_3). ^{31}P{^{1}H} NMR (121 MHz, C$_6$D$_6$) δ 53.36 (s). ^{13}C{^{1}H} NMR (126 MHz, CD$_2$Cl$_2$) δ 225.26 (s), 149.04 (vt, J$_{PC}$ = 14.0 Hz), 141.36 (vt, J$_{PC}$ = 14.3 Hz), 132.80 (s), 132.17 (vt, J$_{PC}$ = 7.0 Hz), 130.66 (s), 128.19 (s), 118.03 (s), 111.15 (s), 26.62 (vt, J$_{PC}$ = 8.4 Hz), 19.33 (s), 18.64 (s). IR (CaF$_2$ window, C$_6$H$_6$, cm^{-1}) ν$_{CO}$: 1901 (s), 1874 (m), 1848 (s), 1843 (w, sh). Anal. Calcd. for: C$_{34}$H$_{40}$FeO$_4$P$_2$Pd$_2$ (**2**) (%): C, 48.42; H, 4.78. Found: C, 48.25; H, 5.08.

Synthesis of Complex 3·[BF₄]

Compound **1** was generated in an analogous fashion to the procedure described in the synthesis of **2** again using 4-bis(2-diisopropylphosphinophenyl)benzene (40 mg, 0.0865 mmol, 1 equiv.) and [Pd(MeCN)$_3$]$_2$[BF$_4$]$_2$ (MeCN = acetonitrile) (54.7 mg, 0.0865 mmol, 1 equiv.). To the *in situ* generated acetonitrile solution of **1** was added Na[Co(CO)4] (16.8 mg, 0.0865 mmol, 1 equiv.) as an acetonitrile solution (*ca.* 2 mL). The reaction mixture was allowed to stir for 1 hr at room temperature. During this time the reaction mixture turned a deep purple-red. The volatiles were then removed under reduced pressure. The residue was then suspended in benzene and collected on a Celite pad. The solid was then washed with additional benzene until the washes became colorless. The washed solid was then dissolved in tetrahydrofuran and filtered through the Celite pad. Removal of volatiles yielded the product as a purple-red solid. Yield: 40 mg, (49 %). Single crystals suitable for X-ray diffraction were grown by the vapor diffusion of hexanes into a concentrated tetrahydrofuran:benzene solution at room temperature. ^{1}H NMR (300 MHz, CD$_3$CN) δ 7.92-7.62 (m, 8H, aryl-H), 6.39 s, 4H, central aryl-H), 2.72 (m, 4H, CH), 1.18 (m, 24H, CH_3). ^{31}P{^{1}H} NMR (121 MHz, CD$_3$CN) δ 61.83 (s). ^{19}F NMR (282 MHz, CD$_3$CN) δ 61.83 (s).^{13}C{^{1}H} NMR (126 MHz, CD$_3$CN) δ 203.70 (broad), 146.58 (vt, J$_{PC}$ = 12.6 Hz), 136.83 (vt, J$_{PC}$ = 17.7 Hz), 133.50 (s), 132.60 (s), 132.23 (s), 129.77 (s), 116.42 (s), 114.30 (s), 26.40 (s), 18.84 (s), 18.04 (s). IR (CaF$_2$ window, THF, cm^{-1}) ν$_{CO}$: 2057 (s), 2012 (m), 1915 (m), 1878 (w, sh). Anal. Calcd. for: C$_{34}$H$_{40}$BCoF$_4$O$_4$P$_2$Pd$_2$ (**3•[BF₄]**) (%): C, 43.76; H, 4.32. Found: C, 43.58; H, 4.48.

Synthesis of Complex 3

Compound **3•[BF₄]** (50 mg, 0.0535 mmol, 1 equiv.) was added to a 20 mL scintillation vial. Tetrahydrofuran (*ca.* 5 mL) was added to fully dissolve **3•[BF₄]**. Cobaltocene (10.1 mg, 0.0535 mmol, 1 equiv.) was added as a tetrahydrofuran solution (1 mL) and the reaction mixture was allowed to stir for 1 hr. During this time the solution changed from purple-red to a green-brown. The volatiles were removed under reduced pressure. The residue was suspended in hexanes and collected over a Celite pad. The solid was washed with hexanes until only a pale green tinge remained in the washes which were initially brown. The remaining green colored material was dissolved in benzene and brought through the Celite pad. The benzene filtrate was then dried to a solid under reduced pressure. The benzene soluble material was then dissolved in minimal

diethyl ether and then several drops of hexamethyldisiloxane were added. The product was then precipitated by the slow evaporation of diethyl ether. Yield: 14 mg (31 %). The product is unstable and prone to decomposition. Therefore characterization was obtained immediately after synthesis. Single crystals were obtained from the vapor diffusion of diethyl ether out of a concentrated solution of **3**. IR (CaF$_2$ window, THF, cm^{-1}) v_{CO}: 2007 (s), 1920 (m, sh), 1879 (m), 1837 (m). Anal. Calcd. for: C$_{34}$H$_{40}$CoO$_4$P$_2$Pd$_2$ (**8**) (%): C, 48.25; H, 4.76. Found: C, 48.24; H, 4.61.

Synthesis of Complex 5

A Schlenk tube fitted with a screw-in Telfon stopper was charged with **4** (100 mg, 0.191 mmol, 1 equiv.) and a magnetic stirbar. [Pd(MeCN)$_3$]$_2$[BF$_4$]$_2$ (MeCN = acetonitrile) (121 mg, 0.191 mmol, 1 equiv.) was transferred as an acetonitrile solution (*ca*. 20 mL) and the mixture was allowed to stir at room temperature for 1 hr. During this the time the reaction mixture became a homogenous deep red. Na$_2$[Fe(CO)$_4$] (40.9 mg, 0.191, 1 equiv.) was then added as a partially solubilized tetrahydrofuran suspension (*ca*. 2 mL) and the reaction was allowed to stir for 1 hr at room temperature. The volatiles were then removed under reduced pressure. The residue was triturated with hexanes and collected over a Celite pad. The solid was then washed with additional hexanes until the washes became colorless. Then 10 mL of cold ether were used to wash the solid. The remaining solid was dissolved in benzene and brought through the Celite pad. Removal of volatiles yielded the product as a red solid. Yield: 40 mg (23 %). Crystals suitable for X-ray diffraction studies were grown from the vapor diffusion of hexanes into a concentrated tetrahydrofuran:benzene (1:1) solution. ^{1}H NMR (300 MHz, C$_6$D$_6$) δ 7.47 (d, J$_{HH}$ = 7.6 Hz, 2H, aryl-*H*), 7.28 (m, 2H, aryl-*H*), 7.20 (m, 2H, aryl-*H*), 7.09 (t, J$_{HH}$ = 7.4 Hz, 2H, aryl-*H*), 5.55 (s, 2H, central aryl-*H*), 2.94 (s, 6H, OC*H*$_3$), 2.40 (m, 2H, C*H*), 2.27 (m, 2H, C*H*), 1.33 (m, 12H, C*H*$_3$), 0.99 (aq, J$_{HH}$ = 7.2 Hz, 6H, C*H*$_3$), 0.91 (aq, J$_{HH}$ = 7.2 Hz, 6H, C*H*$_3$). ^{31}P{^{1}H} NMR (121 MHz, C$_6$D$_6$) δ 56.92 (s). ^{13}C{^{1}H} NMR (126 MHz, CD$_2$Cl$_2$) δ 225.48 (s), 147.08 (vt, J$_{PC}$ = 14.7 Hz), 143.24 (vt, J$_{PC}$ = 15.0 Hz), 140.86 (s), 132.70 (s), 132.20 (vt, J$_{PC}$ = 7.6 Hz), 130.83 (s), 128.05 (s), 54.90 (s), 26.84 (d, J$_{PC}$ = 8.6 Hz), 26.71 (d, J$_{PC}$ = 8.4 Hz), 19.56 (vt, J$_{PC}$ = 5.1 Hz), 19.41 (vt, J$_{PC}$ = 4.6 Hz), 18.77 (s), 18.53 (s). IR (CaF$_2$ window, C$_6$H$_6$, cm^{-1}) v_{CO}: 1898, 1867, 1838 (fourth IR stretch likely coincidentally underneath 1838 band by analogy to the IR of compound **2**). Anal. Calcd. for: C$_{36}$H$_{44}$FeO$_6$P$_2$Pd$_2$ (**5**) (%): C, 47.86; H, 4.91. Found: C, 48.14 H, 4.86.

Synthesis of Complex 7

A Schlenk tube fitted with a screw-in Teflon stopper was charged with **6** (300 mg, 0.462 mmol, 1 equiv.) and a magnetic stirbar. Tetrahydrofuran (*ca*. 20 mL) was then transferred to the Schlenk tube to yield a green homogeneous solution. Na$_2$[Fe(CO)$_4$] (100.7 mg, 0.462 mmol, 1 equiv.) was added as a partially solubilized tetrahydrofuran suspension (*ca*. 10 mL). This addition resulted in an immediate color change from green to brown within a minute. The reaction mixture was allowed to stir at room temperature for 1 hr. Volatiles were then removed under reduced pressure. The dark brown residue was suspended in hexanes and filtered on a Celite pad. The solid was then washed with hexanes until the washes were colorless. The remaining solid was then washed with 10 mL cold diethyl ether. Finally, the product was dissolved with benzene and brought through the Celite pad. The benzene soluble material was lyophilized to yield the product

as a brown powder. Yield: 160 mg (41 %). Crystals suitable for X-ray diffraction studies could be grown from the slow vapor diffusion of hexanes into a concentrated tetrahydrofuran:benzene (1:1) solution. However, the compound decomposes in solution over extended periods of time and the cleanest material was obtained without crystallization. ^{1}H NMR (300 MHz, C_6D_6) δ 7.17 (d, J_{HH} = 7.4 Hz, 2H, aryl-H), 7.05-6.90 (m, 6H, aryl-H), 5.78 (s, 4H, central aryl-H), 2.32 (h, J_{HH} = 7.0 Hz, 4H, CH), 1.19 (m, 12H, CH_3), 0.89 (aq, J_{HH} = 7.0 Hz, CH_3). ^{31}P{^{1}H} NMR (121 MHz, C_6D_6) δ 43.18 (s). ^{13}C{^{1}H} NMR (126 MHz, C_6D_6) δ 225.38 (broad s), 150.24 (vt, J_{PC} = 14.2 Hz), 138.27 (vt, J_{PC} = 15.0 Hz), 131.40 (s), 130.23 (s), 130.09 (s), 127.70 (s), 103.31 (s), 102.02 (s), 25.18 (vt, J_{PC} = 9.7 Hz), 18.60 (s), 17.66 (s). IR (CaF$_2$ window, C_6H_6, cm^{-1}) ν$_{CO}$: 1896, 1874, 1821, 1798.3 (sh). Anal. Calcd. for: $C_{34}H_{40}FeO_4P_2Ni_2$ (**7**) (%): C, 54.60; H, 5.39. Found: C, 54.69; H, 5.35.

Nuclear Magnetic Resonance Spectra
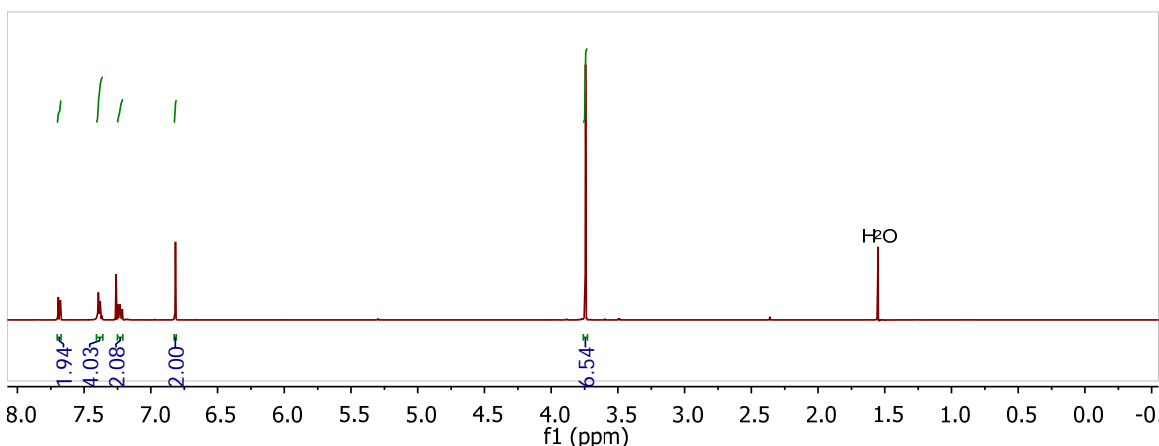
Figure S1. ^{1}H-NMR (500 MHz, CDCl$_3$) spectrum of **A**.
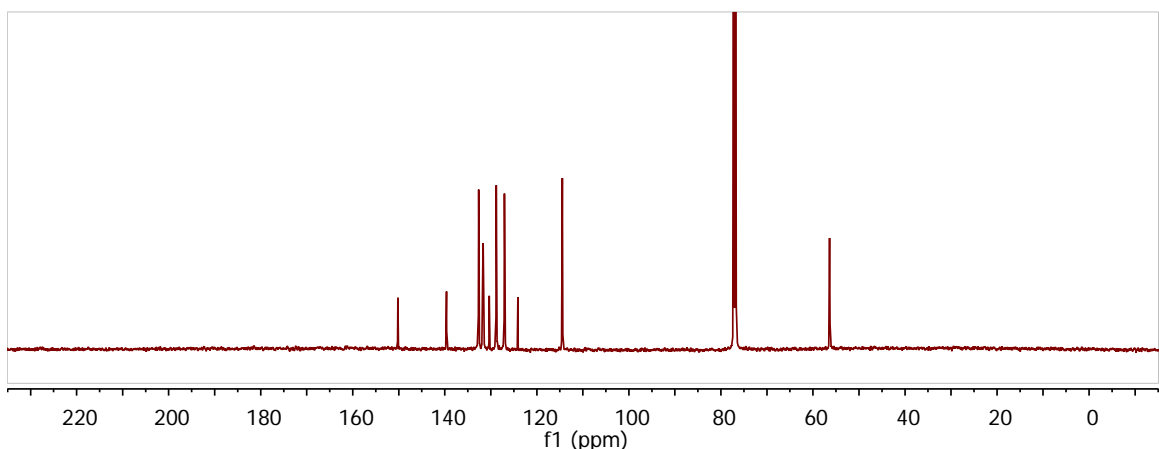
Figure S2. ^{13}C{^{1}H}-NMR (126 MHz, CDCl$_3$) spectrum of **A**.
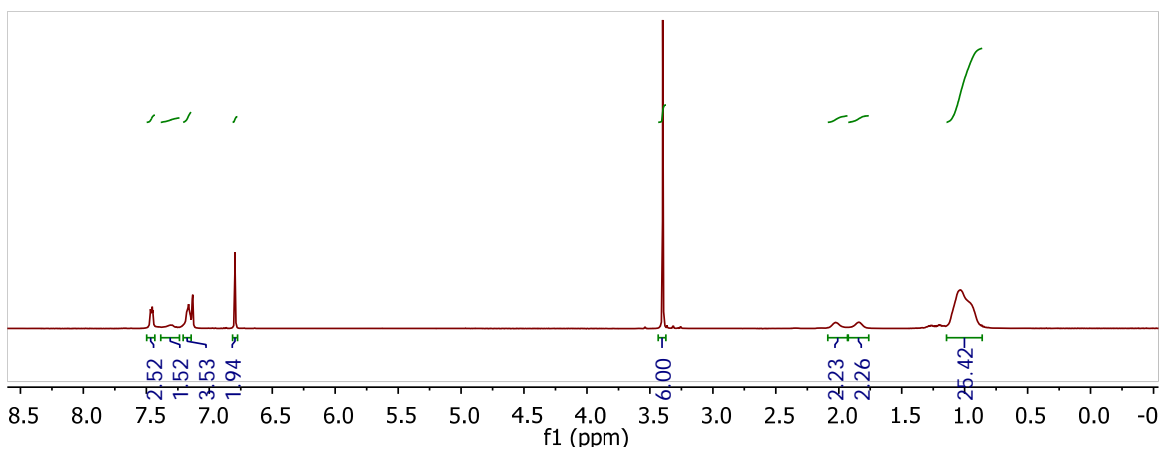
Figure S3. ^{1}H-NMR (500 MHz, C$_6$D$_6$) spectrum of **4**.
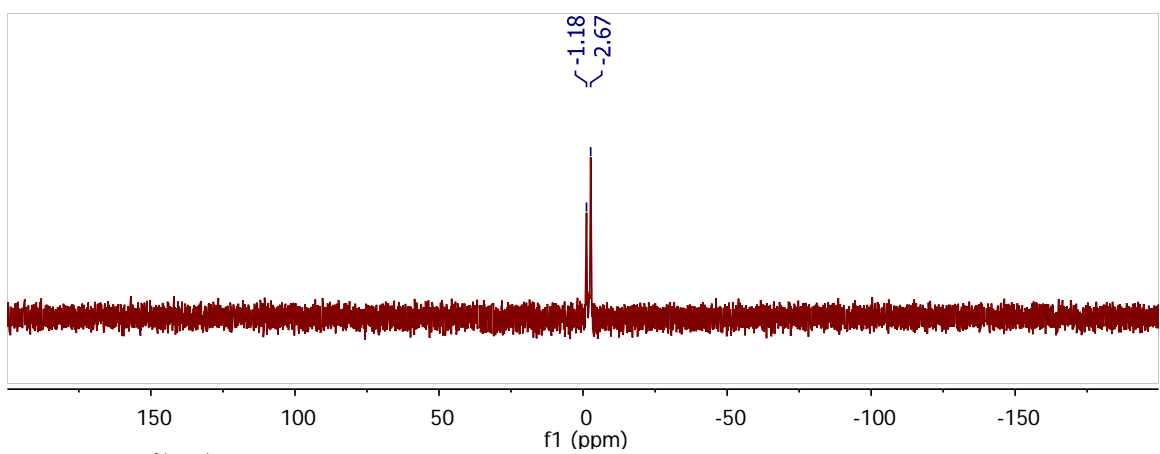
Figure S4. ^{31}P{^{1}H}-NMR (121 MHz, C$_6$D$_6$) spectrum of **4**.
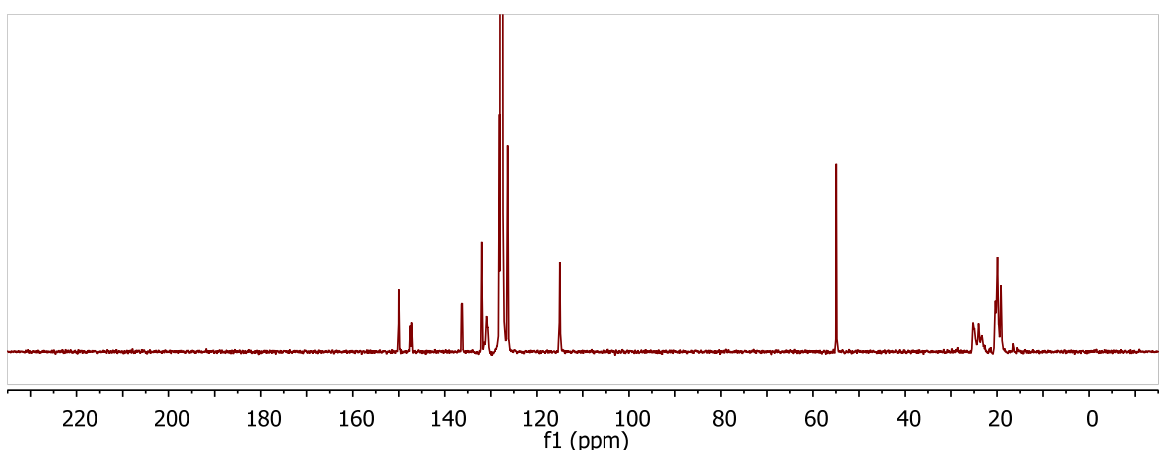
Figure S5. ^{13}C{^{1}H}-NMR (126 MHz, C$_6$D$_6$) spectrum of **4**.
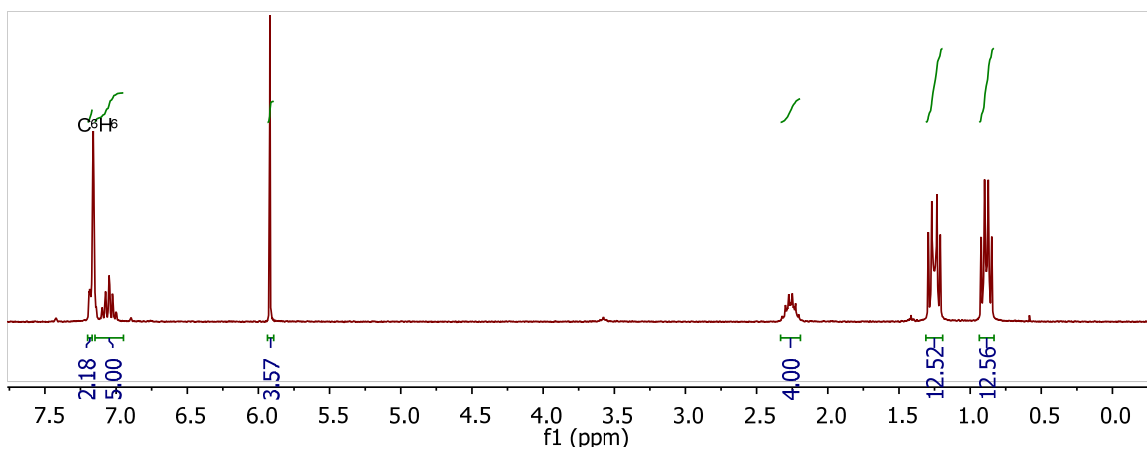
Figure S6. ^{1}H-NMR (300 MHz, C$_6$D$_6$) spectrum of complex **2**.
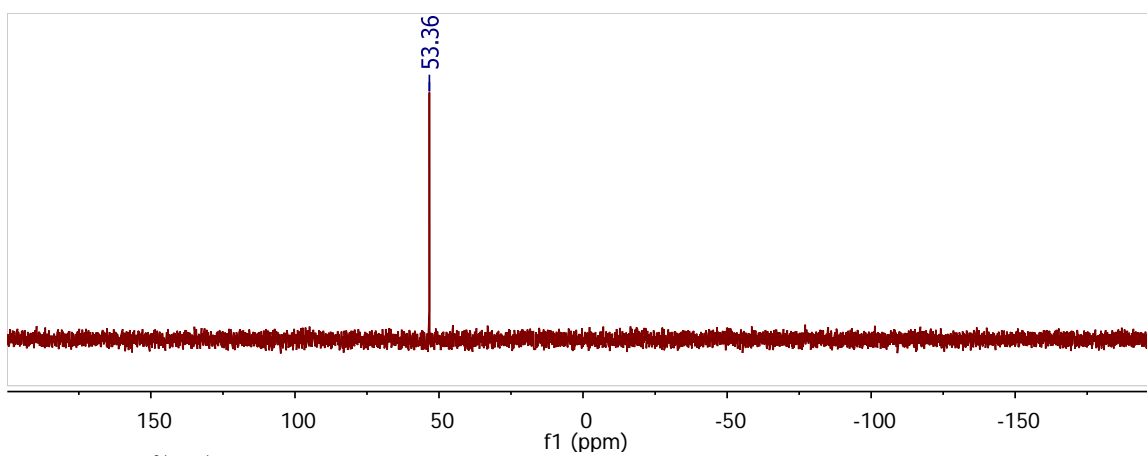
Figure S7. ^{31}P{^{1}H}-NMR (121 MHz, C$_6$D$_6$) spectrum of complex **2**.
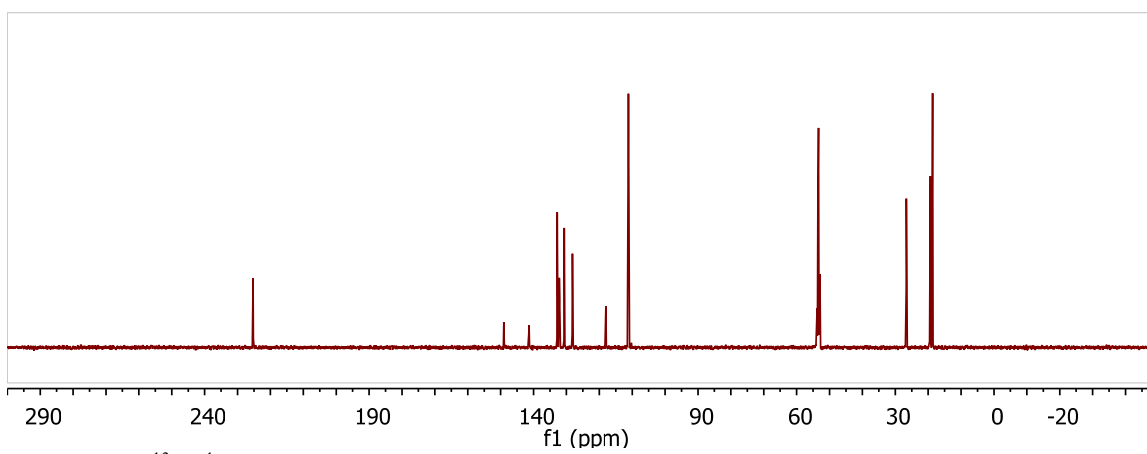
Figure S8. ^{13}C{^{1}H}-NMR (126 MHz, CD$_2$Cl$_2$) spectrum of complex **2**.
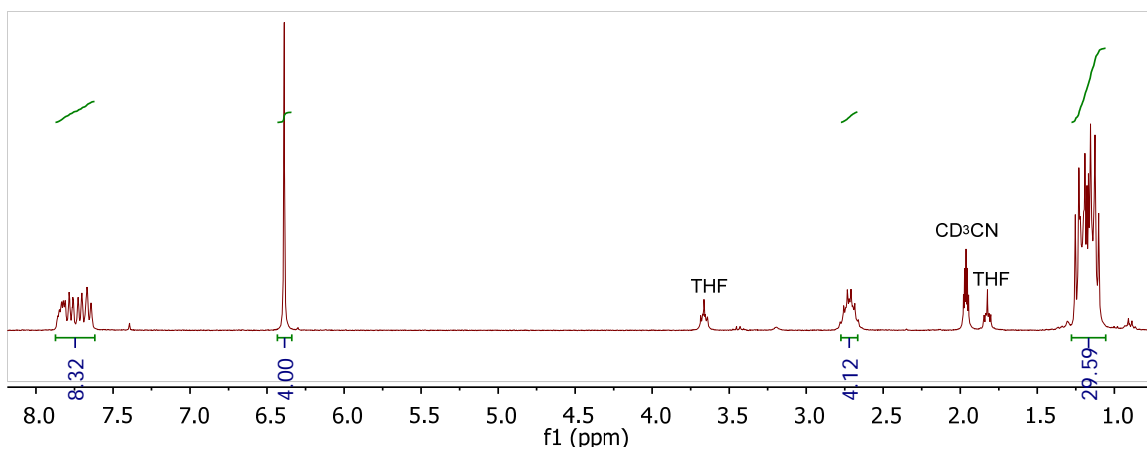
Figure S9. ^{1}H-NMR (300 MHz, CD$_3$CN) spectrum of complex **3•[BF$_4$]**.
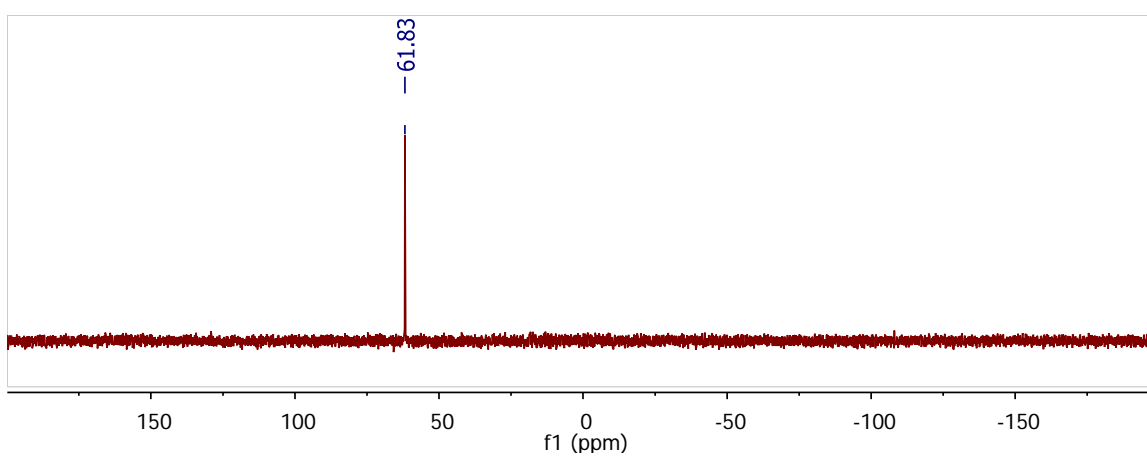
Figure S10. ^{31}P{^{1}H}-NMR (121 MHz, CD$_3$CN) spectrum of complex **3•[BF$_4$]**.
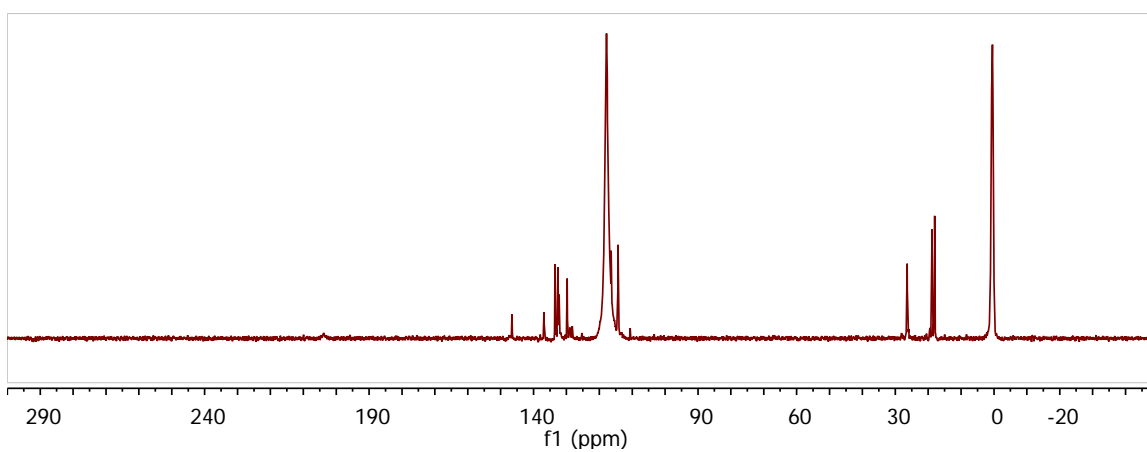
Figure S11. ^{13}C{^{1}H}-NMR (126 MHz, CD$_3$CN) spectrum of complex **3•[BF$_4$]**.
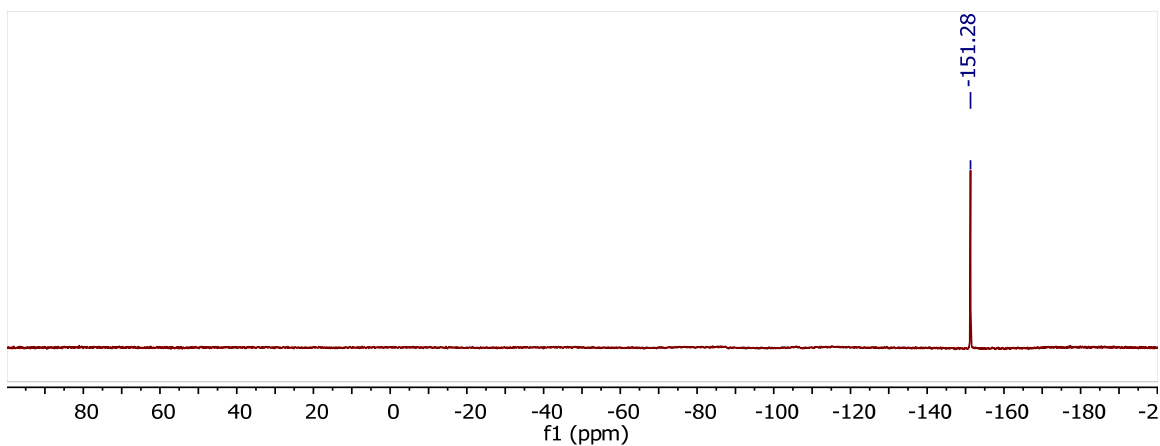
Figure S12. ^{19}F-NMR (282 MHz, CD$_3$CN) spectrum of complex **3•[BF$_4$]**.
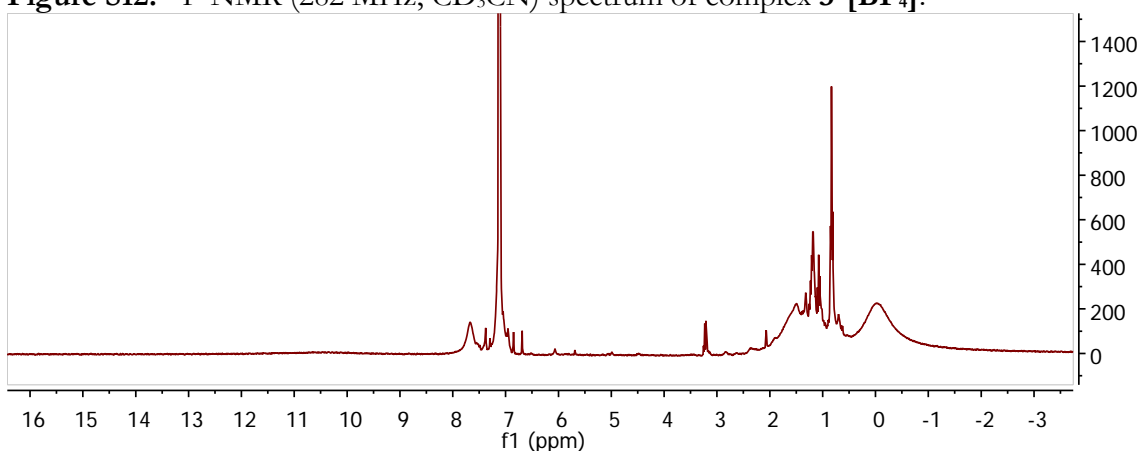
Figure S13. ^{1}H-NMR (300 MHz, C$_6$D$_6$) spectrum of complex **3**.
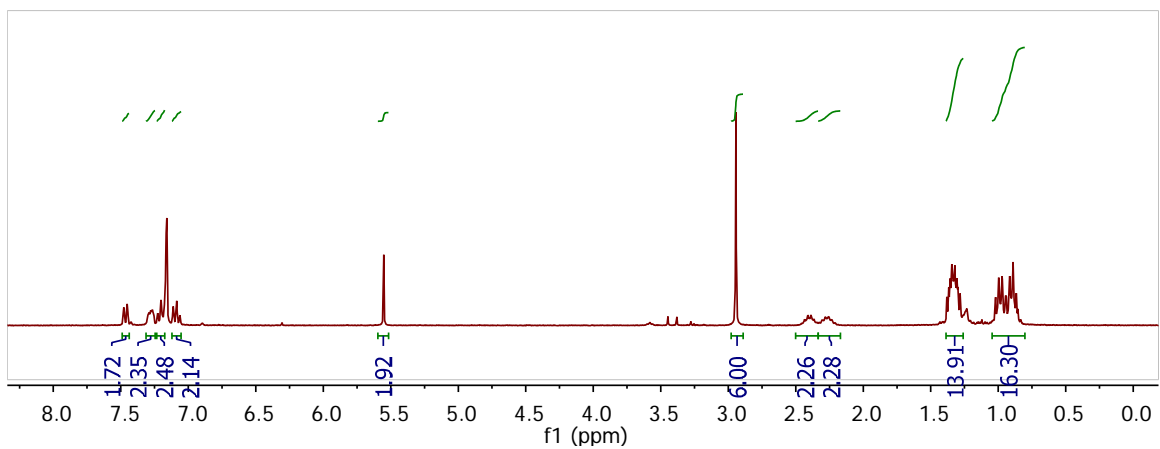
Figure S14. ^{1}H-NMR (300 MHz, C$_6$D$_6$) spectrum of complex **5**.
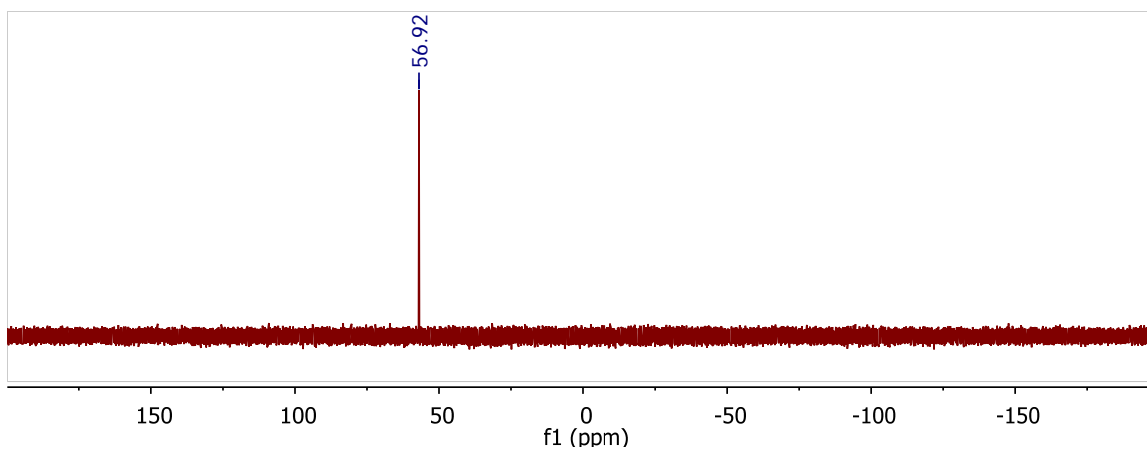
Figure S15. $^{31}P\{^{1}H\}$-NMR (121 MHz, C_6D_6) spectrum of complex **5**.
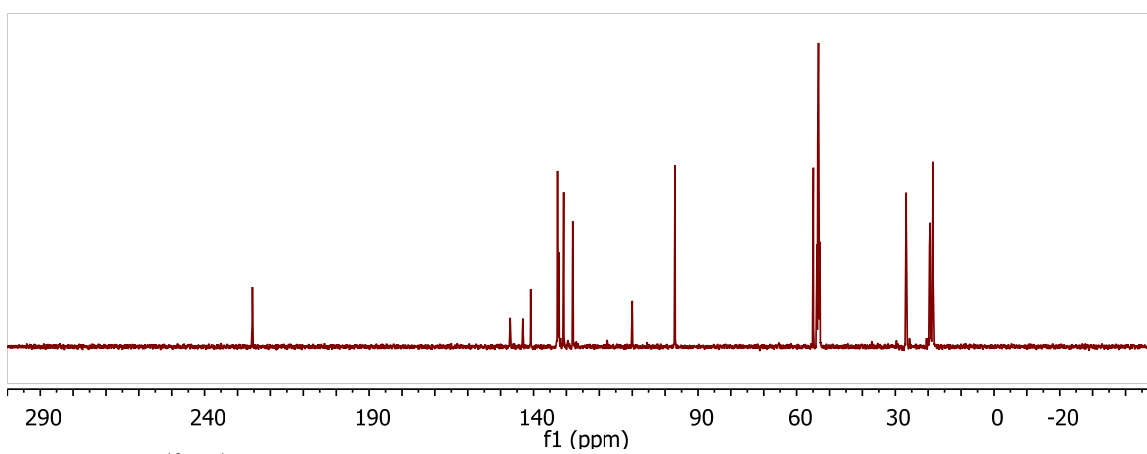
Figure S16. $^{13}C\{^{1}H\}$-NMR (126 MHz, CD_2Cl_2) spectrum of complex **5**.
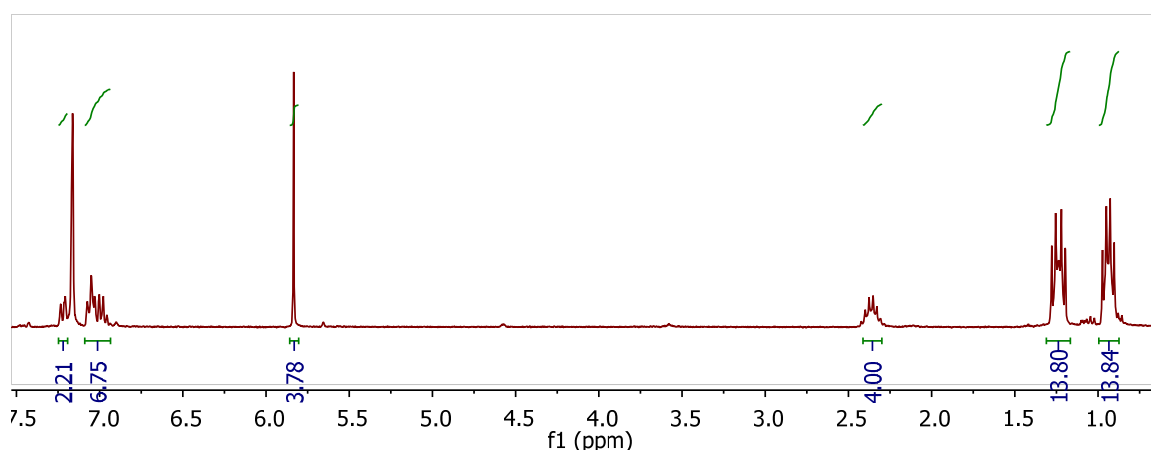
Figure S17. ^{1}H-NMR (300 MHz, C_6D_6) spectrum of complex **7**.
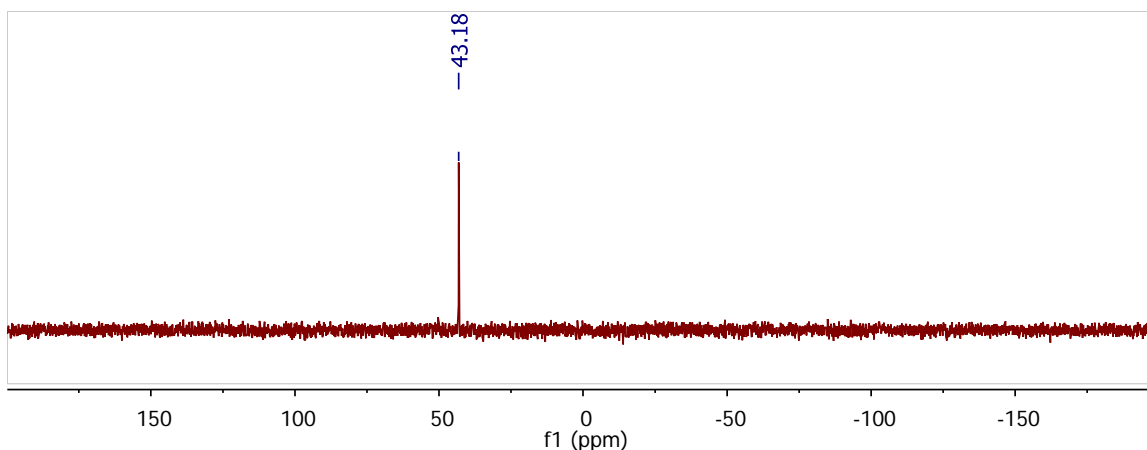
Figure S18. $^{31}P\{^1H\}$-NMR (121 MHz, C_6D_6) spectrum of complex **7**.
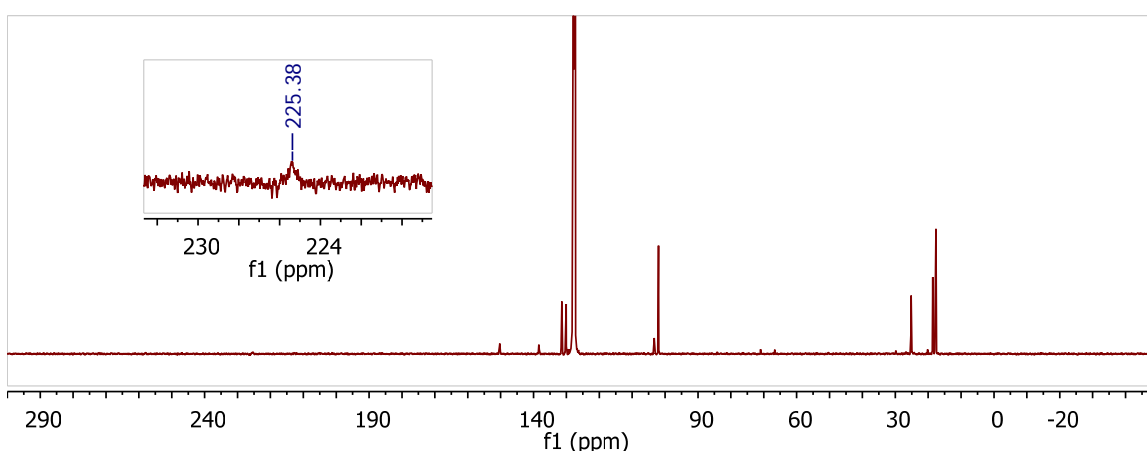

Figure S19. $^{13}C\{^1H\}$-NMR (126 MHz, C_6D_6) spectrum of complex **7**.

Electrochemistry Details

Electrochemical measurements of complex **2**, **3•[BF₄]**, **5,** and **7** were taken on a Pine Instrument Company biopotentiostat model AFCBP1 as 3 millimolar solutions in tetrahydrofuran using 0.1 molar [*n*Bu₄N][PF₆] as the electrolyte with a platinum wire counter electrode, a glassy carbon working electrode, and a silver/silver nitrate reference electrode in 0.1 molar [*n*Bu₄N][PF₆] as an acetonitrile solution. Electrochemical measurements of compounds were internally referenced to ferrocene.
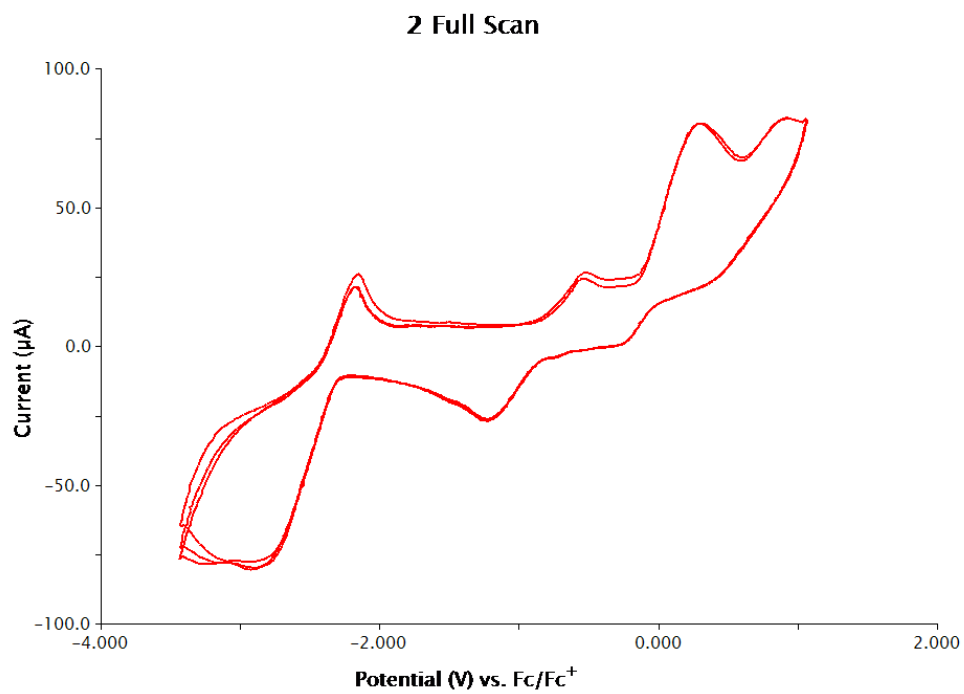
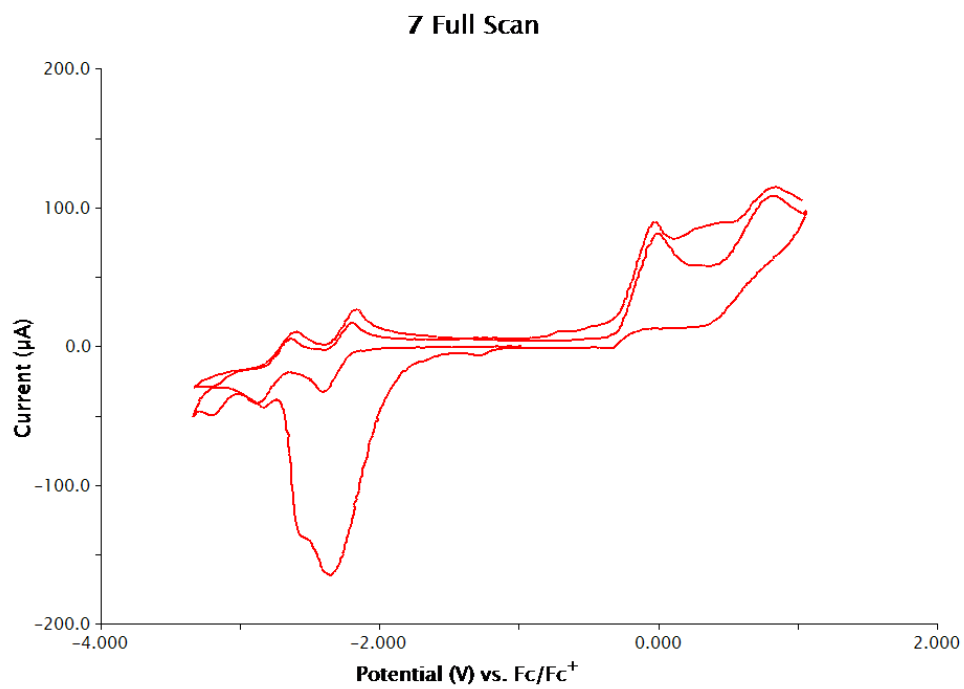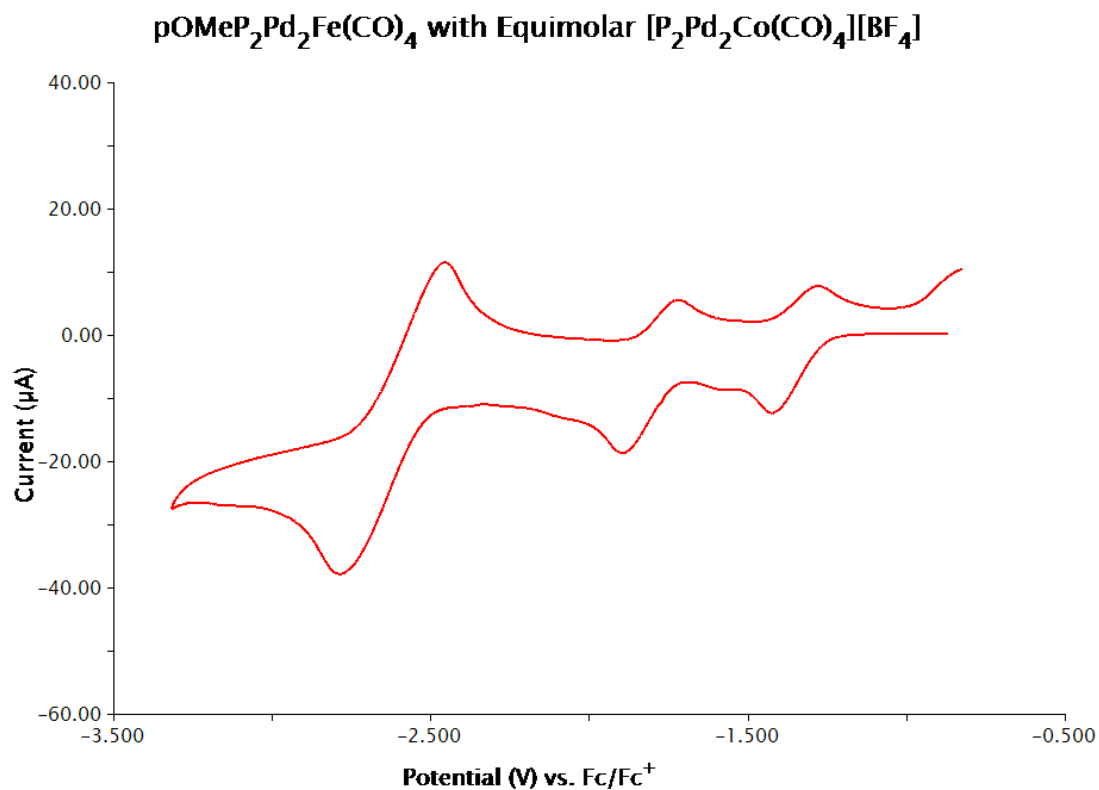**Figure S20.** Complex **2** full cyclic voltammogram.
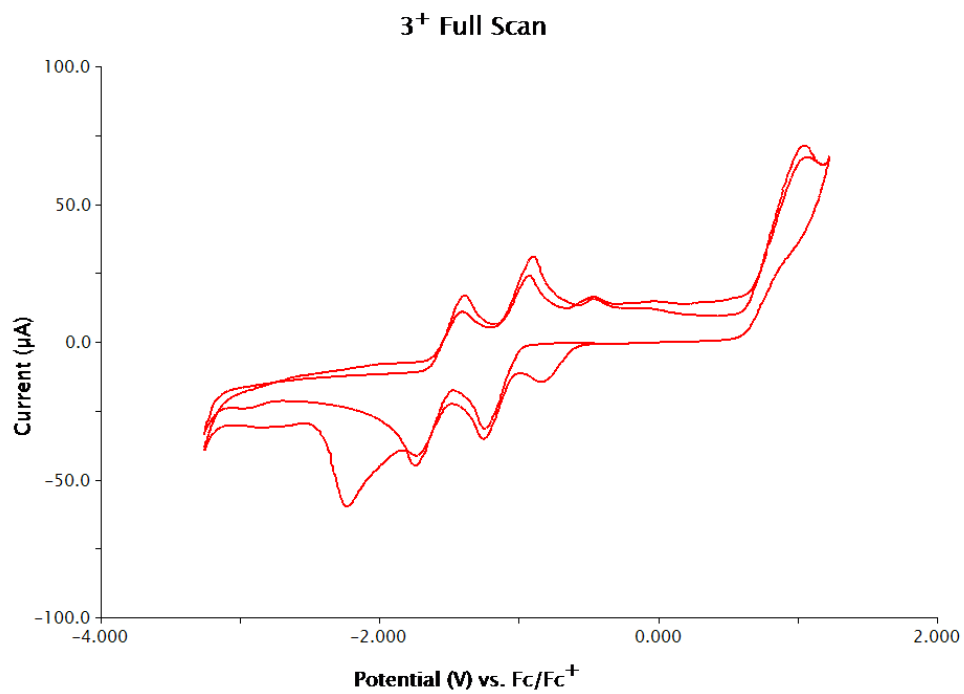
Figure S21. Complex **3·[BF₄]** full cyclic voltammogram.

5 Full Scan
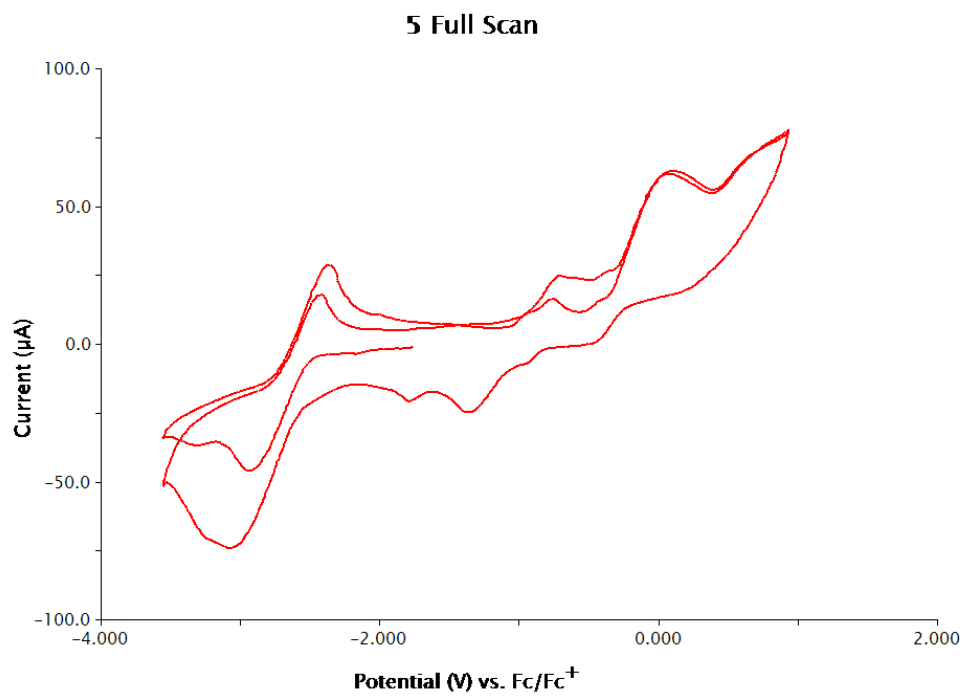
Figure S22. Complex **5** full cyclic voltammogram.

7 Full Scan

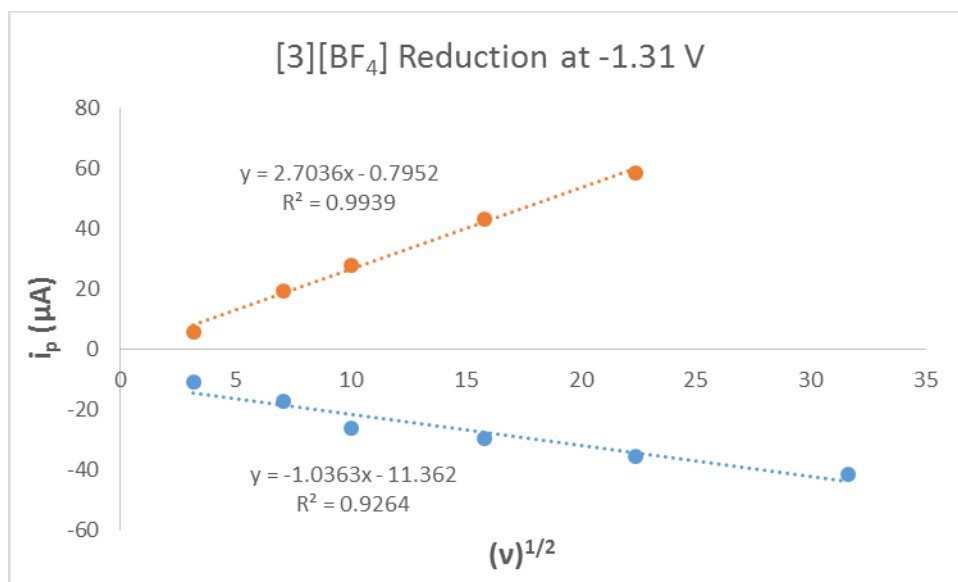
Figure S23. Complex **7** full cyclic voltammogram.

Figure S24. Complex **5** and **3·[BF₄]** reductive scan as equimolar solution.
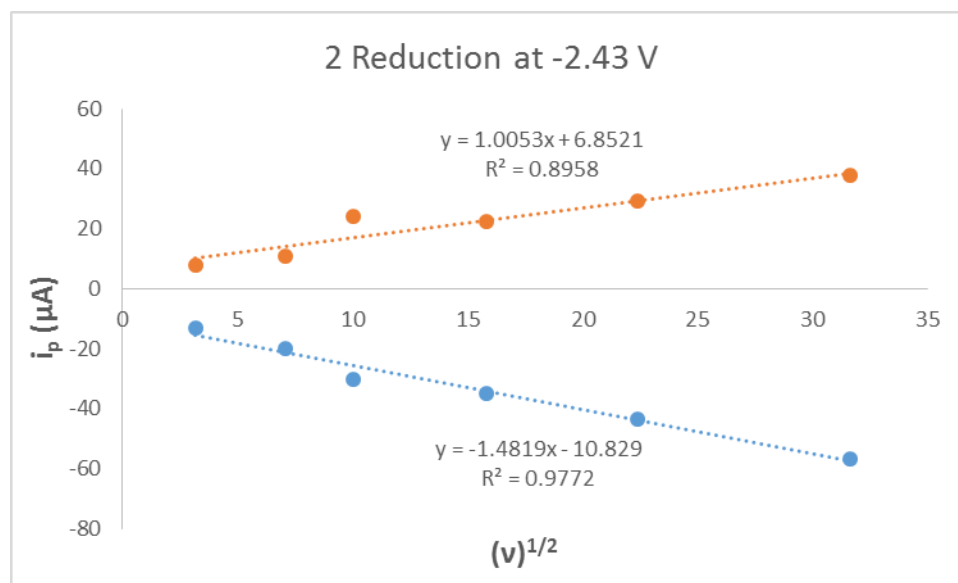
Figure S25. Plot of the scan rate dependence for the reduction of compound **2** with the cathodic (blue) and anodic scans (orange)

Figure S26. Plot of the scan rate dependence for the first reduction of compound **3·[BF₄]** with the cathodic (blue) and anodic scans (orange)

Figure S27. Plot of the scan rate dependence for the second reduction of compound **3·[BF₄]** with the cathodic (blue) and anodic scans (orange)
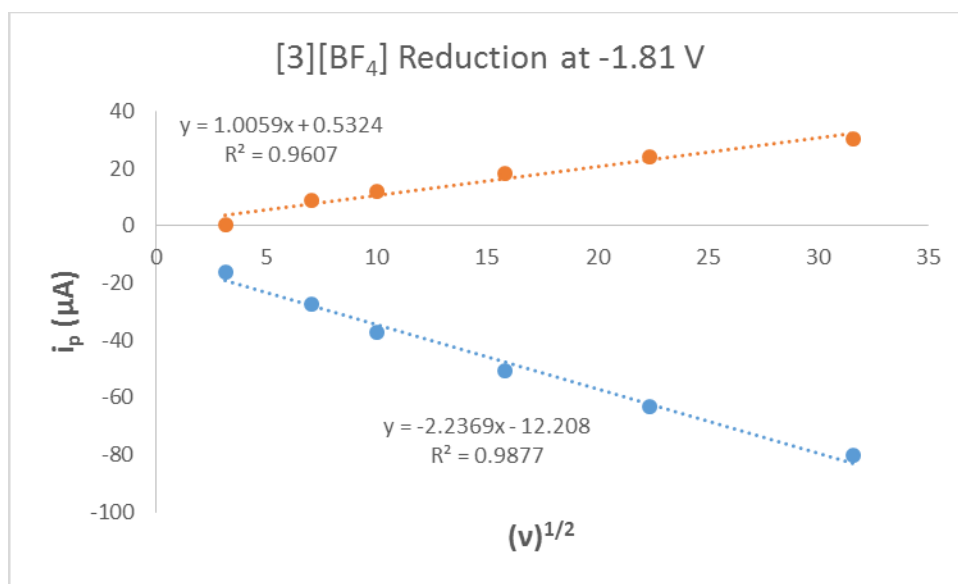
Figure S28. Plot of the scan rate dependence for the reduction of compound **5** with the cathodic (blue) and anodic scans (orange)

Figure S29. Plot of the scan rate dependence for the first reduction of compound **7** with the cathodic (blue) and anodic scans (orange)

7 Reduction at -2.75 V

$y = 2.5658x + 0.0213$
$R^2 = 0.9961$
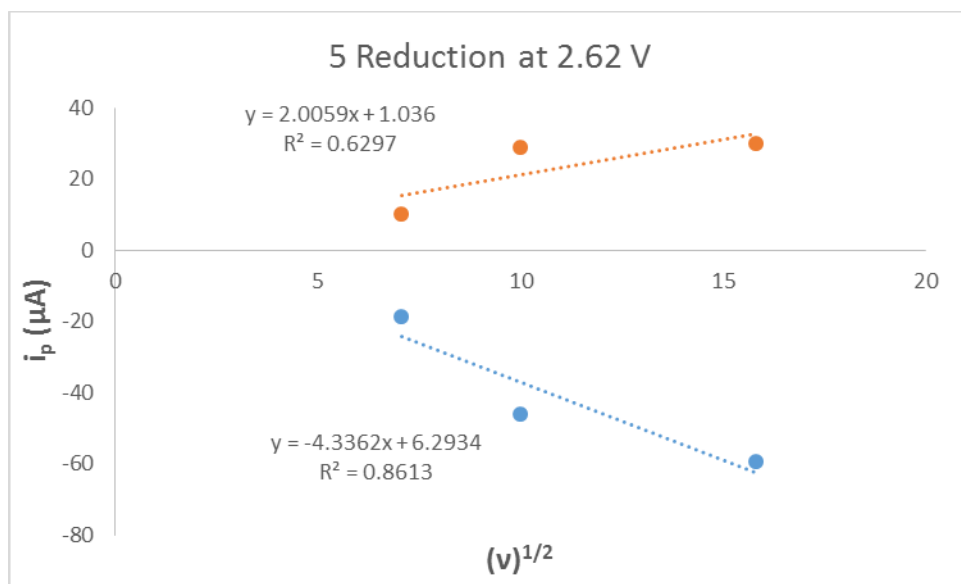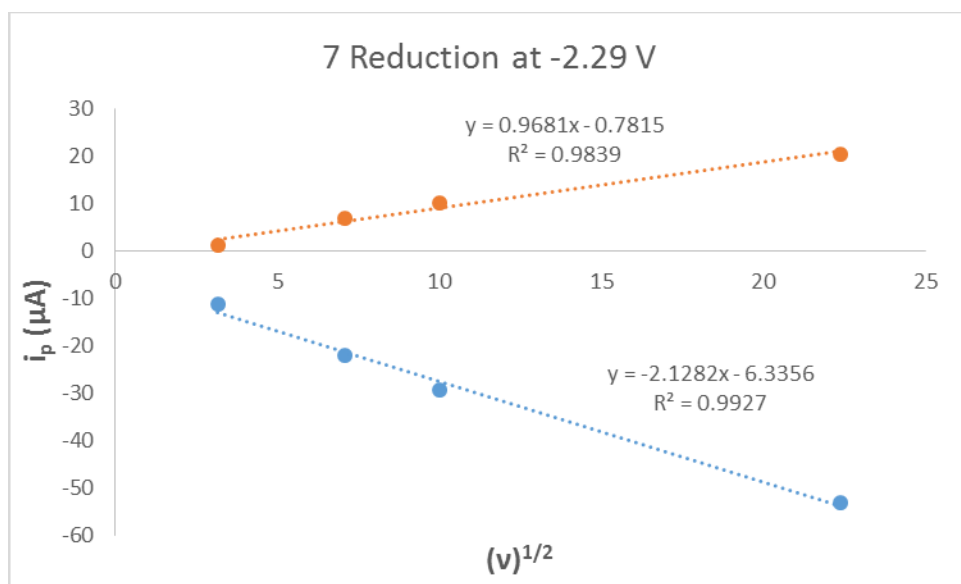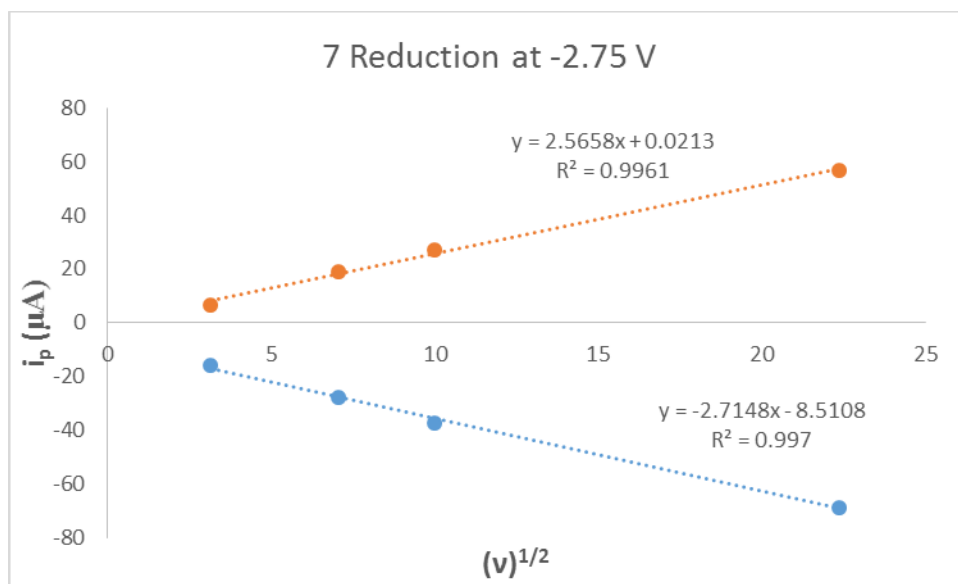
$y = -2.7148x - 8.5108$
$R^2 = 0.997$

i_p (µA)

$(v)^{1/2}$

Figure S30. Plot of the scan rate dependence for the second reduction of compound **7** with the cathodic (blue) and anodic scans (orange)
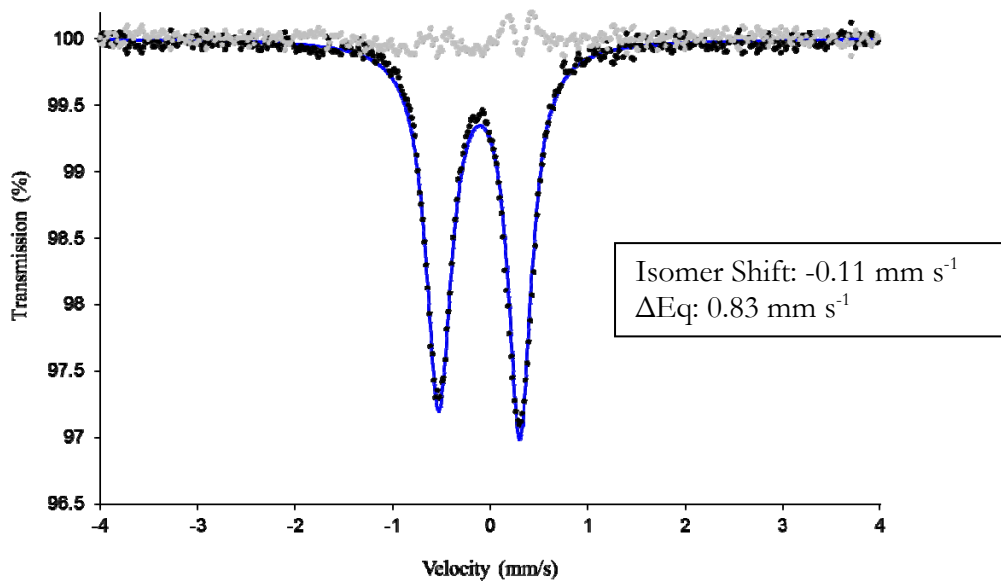
Mössbauer Details

Spectra were recorded on a spectrometer from SEE Co. operating in the constant acceleration mode in a transmission geometry. Spectra were recorded with the temperature of the sample maintained at 80 K. The sample was kept in an SVT-400 Dewar from Janis, at zero field. Application of a magnetic field of 54 mT parallel to the γ-beam did not cause detectable changes in the spectra recorded at 80 K. The quoted isomer shifts are relative to the centroid of the spectrum of a metallic foil of α-Fe at room temperature. Samples were prepared by grinding polycrystalline material into a fine powder and then mounted in a cup fitted with a screw cap as a boron nitride pellet. Data analysis was performed using the program WMOSS (www. wmoss.org) and quadrupole doublets were fit to Lorentzian lineshapes.

Isomer Shift: -0.10 mm s^{-1}
ΔEq: 1.08 mm s^{-1}
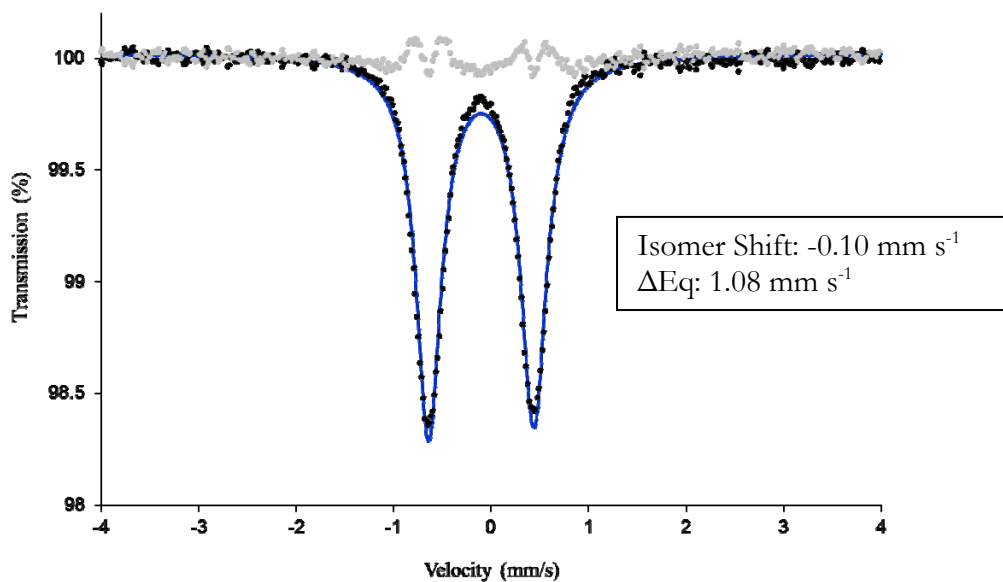
Figure S31. Zero-field ^{57}Fe Mössbauer spectrum for **2**, 80 K. Data: black dots; spectral fit: blue line; and residual: grey dots.

Isomer Shift: -0.09 mm s^{-1}
ΔEq: 1.13 mm s^{-1}
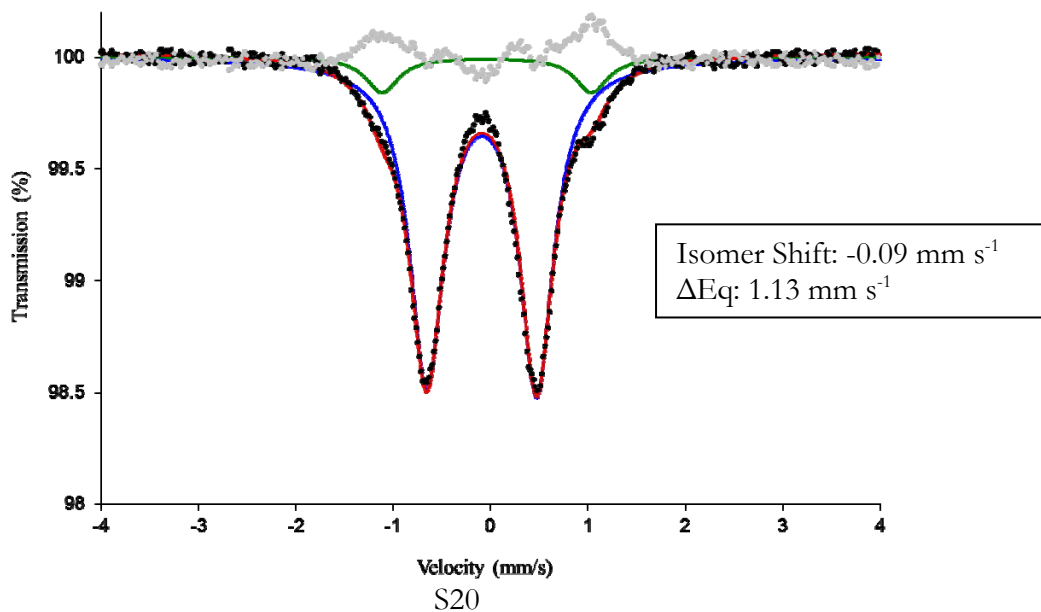
Figure S32. Zero-field ^{57}Fe Mössbauer spectrum for **5** and minor decomposition (green line) following removal from glovebox, 80 K. Data: black dots; spectral fit: red line; deconvolution: blue and green lines; residual: grey dots.
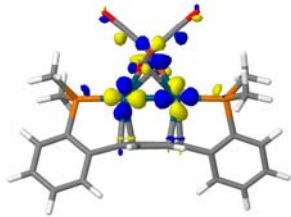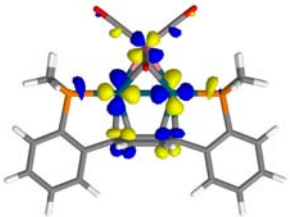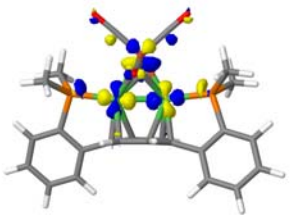

Isomer Shift: -0.11 mm s^{-1}
ΔEq: 0.83 mm s^{-1}
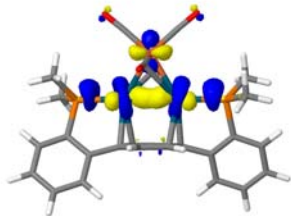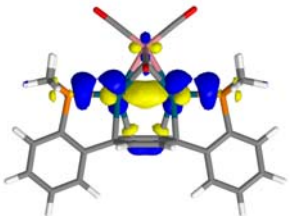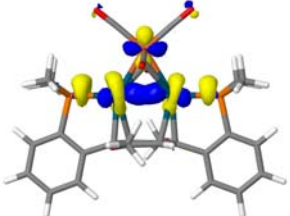
Figure S33. Zero-field ^{57}Fe Mössbauer spectrum for **7**, 80 K. Data: black dots; spectral fit: blue line; and residual: grey dots.
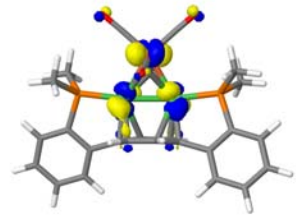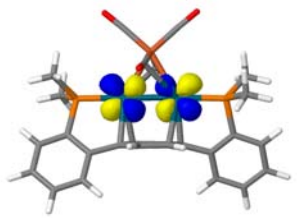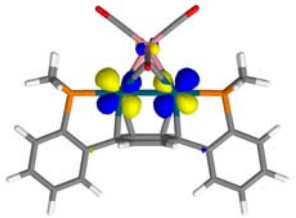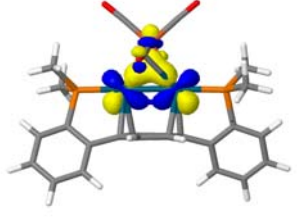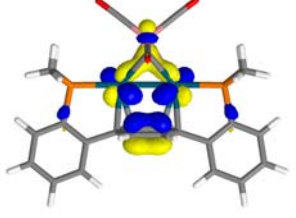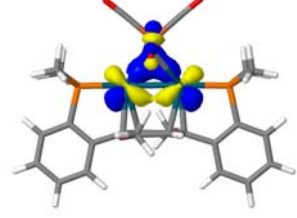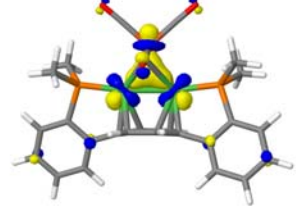
Computational Details

All calculations were performed with DFT as implemented in Gaussian 09 Revision C.01.[8] Geometry optimizations and electronic structure calculations were performed with the TPSSh hybrid functional[9] that, incorporating 10% exact exchange (c.f. BLYP 0% and B3LYP 20%), has been shown to be effective for calculating transition metal-containing compounds.[10] The LANL2DZ basis set and effective core potential[11] for Pd atoms and the 6-31++G(d,p) basis set[12] for all other atoms was used. No solvent corrections were used. For all compounds isopropyl substituents on the phosphine ligands were truncated to methyl groups and have been designated with the -Me$_2$ suffix to the appropriate compound numbers. Geometry optimizations of **2-Me$_2$** and **7-Me$_2$** were performed under the C$_2$ point group, while **3·[BF$_4$]-Me$_2$** and **5-Me$_2$** were optimized without symmetry constraints. Optimization stationary points were confirmed with subsequent frequency calculations that did not r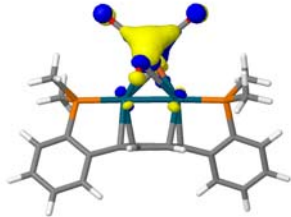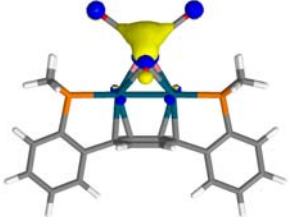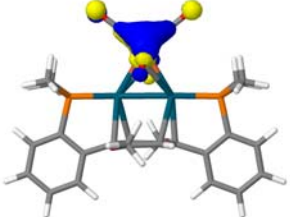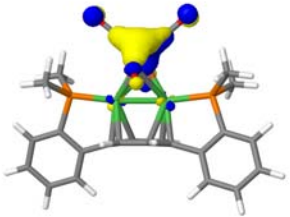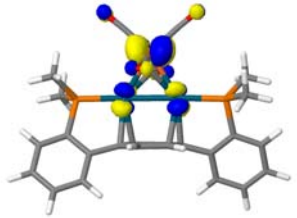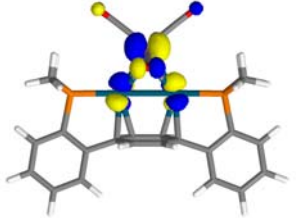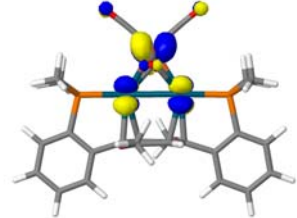eturn imaginary frequency vibrations < -10 cm^{-1}. All molecular orbital illustrations are depicted with a 0.05 isosurface value.
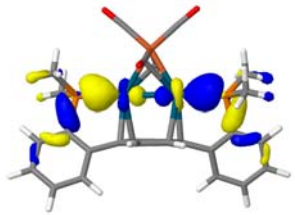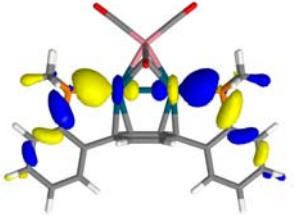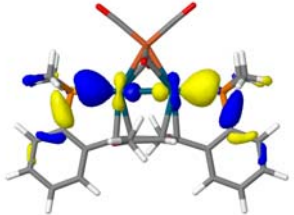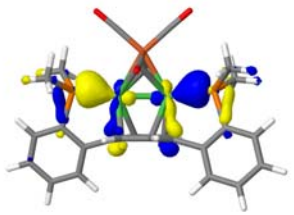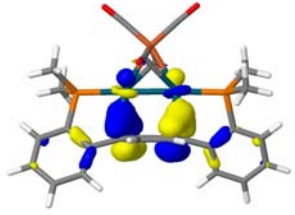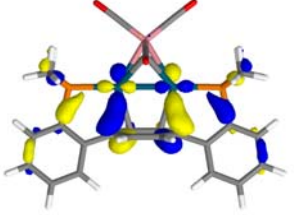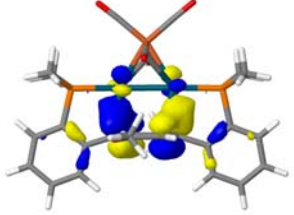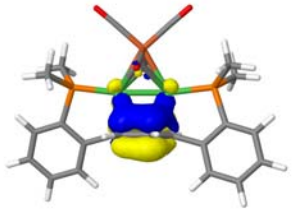
Natural bond order (NBO) calculations were performed to elucidate the nature of the M-M' interactions. There is an unresolved error with NBO3, as implemented in Gaussian09[8], when trying to do bonding analysis of these compounds. So to perform NBO bond analysis, the following procedure was used: the atomic coordinates from the Gaussian09 geometry optimizations were used to run single-point calculations in Orca (version 3.0.3[13]), and Orca was used to generate input files (*.47) for NBO6 [14] analysis. The NBO6 input files were modified by including the keywords BNDIDX and PLOT and listing analogous connectivity patterns in a $CHOOSE block before running. The natural localized molecular orbitals (NLMOs) were visualized using the pre-orthogonalized natural atomic orbitals basis set by opening the *.38 NBO6 output files with JMol.

Table 1. Select Molecular Orbital Illustrations for **2-Me₂**, **3⁺-Me₂**, **5-Me₂**, and **7-Me₂**

2-Me₂	3⁺-Me₂	5-Me₂	7-Me₂	Rep. MO
LUMO	LUMO	LUMO	LUMO	M-M and M-M' antibonding
HOMO-2	HOMO	HOMO-2	HOMO-1	M-M σ-bonding
HOMO-4	HOMO-5	HOMO-4	HOMO-4	M'-CO backbonding

				M-M' π antibonding and M-M δ antibonding
HOMO-5	HOMO-16	HOMO-5	HOMO-7	
HOMO-10	HOMO-13	HOMO-10	HOMO-9	M-M π-antibonding
HOMO-17	HOMO-18	HOMO-18	HOMO-17	M-M and M-M' bonding

HOMO-19	HOMO-17	HOMO-20	HOMO-18	M-P bonding
HOMO-20	HOMO-23	HOMO-21	HOMO-19	M-arene bonding

Table S2. Comparison of Calculated and Experimental IR Parameters

Complex	ν_{CO}(calc) (cm^{-1})	Average ν_{CO}(calc) (cm^{-1})	ν_{CO}(expt) (cm^{-1})	Average ν_{CO}(expt) (cm^{-1})
2	2029.2, 1980.3, 1948.4, 1927.5	1971.4	1901 (s), 1874 (m), 1848 (s), 1843 (w, sh)	1867
3·[BF$_4$]	2110.7, 2076.0, 2023.8, 1991.2	2050.4	2057 (s), 2012 (m), 1915 (m), 1878 (w, sh)	1966
5	2024.3, 1976.3, 1931.4, 1909.3	1960.3	1898 (s), 1867 (m) 1838 (s, coincidental overlap with weak should stretch)	1860
7	2015.0, 1964.1, 1924.7, 1902.8	1951.7	1896 (s), 1874 (m) 1821 (m), 1798 (w, sh)	1847

Table S3. Comparison of Calculated and Experimental Structural Parameters

Complex	d(M-M)$_{calc}$ (Å)	d(M-M')$_{calc}$ (Å)	d(M-M)$_{expt}$ (Å)	d(M-M')$_{expt}$ (Å)
2	2.5889	2.5379, 2.5382	2.5643(3)	2.5374(3)
3·[BF$_4$]	2.5983	2.5463, 2.5464	2.5853(3)	2.6077(3), 2.5472(4)
5	2.5988	2.5398, 2.5402	2.5776(3)	2.5512(6), 2.5541(6)
7	2.3474	2.3970, 2.3976	2.3931(8)	2.4169(6)
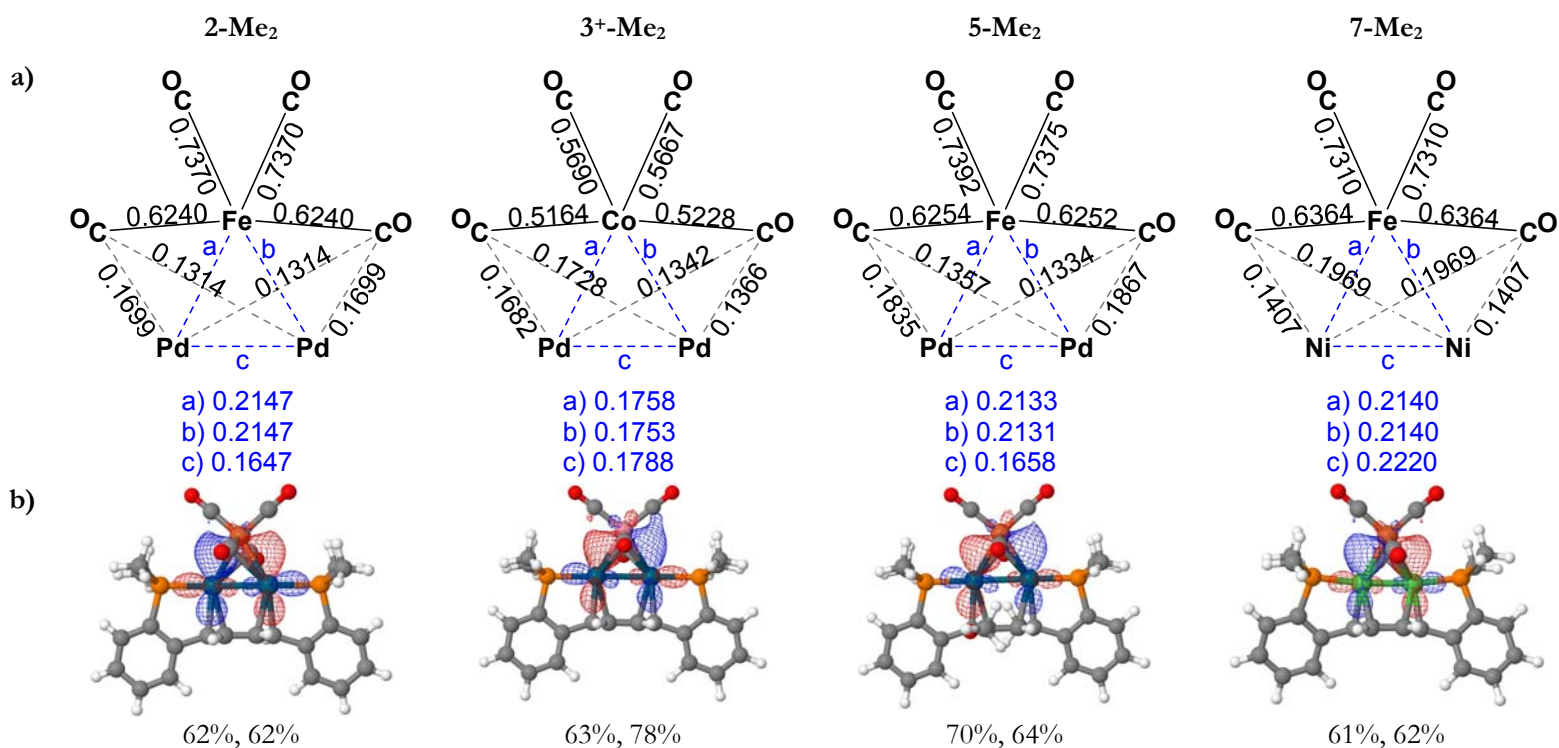
Figure S34. a) Metal–metal and metal-CO Wiberg bond indices and b) (group 10 metal center)–(apical metal center) (M–M') natural localized molecular orbitals (NLMOs) and their contributions to total M–M' bond orders

Crystallographic Information

CCDC 1056167-1056171 contain the supplementary crystallographic data for this paper. These data can be obtained free of charge from The Cambridge Crystallographic Data Centre via www.ccdc.cam.ac.uk/data_request/cif.

Refinement details

In each case, crystals were mounted on a glass fiber or nylon loop using Paratone oil, then placed on the diffractometer under a nitrogen stream. Low temperature (100 K) X-ray data were obtained on a Bruker APEXII CCD based diffractometer (Mo sealed X-ray tube, K_α = 0.71073 Å). All diffractometer manipulations, including data collection, integration and scaling were carried out using the Bruker APEXII software.[15] Absorption corrections were applied using SADABS.[16] Space groups were determined on the basis of systematic absences and intensity statistics and the structures were solved by direct methods using XS (incorporated into SHELXTL) and refined by full-matrix least squares on F^2. All non-hydrogen atoms were refined using anisotropic displacement parameters. Hydrogen atoms were placed in idealized positions and refined using a riding model. The structure was refined (weighted least squares refinement on F^2) to convergence.

Table S4. Crystal and refinement data for reported complexes.

Complex	**2**	**3•[BF$_4$]**	**3**	**5**	**7**
empirical formula	$C_{17}H_{20}Fe_{0.50}O_2P$ Pd	$C_{40}H_{47.50}BCoF_4$ $N_{1.50}O_4P_2Pd_2$	$C_{34}H_{40}CoO_4P_2$ Pd$_2$	$C_{36}H_{44}FeO_6P_2$ Pd$_2$	$C_{17}H_{20}Fe_{0.50}Ni$ O$_2$P
formula wt	421.62	1033.77	846.33	903.30	373.93
T (K)	100	100	100	100	100
a, Å	11.4622(6)	15.9326(8)	15.7355(5)	14.0587(5)	11.5996(6)
b, Å	13.3606(7)	16.5136(9)	13.6086(4)	14.2422(5)	13.1456(7)
c, Å	11.1153(5)	18.4384(10)	15.8392(5)	18.4208(6)	10.9589(5)
α, deg	90	90.490(3)	90	90	90
β, deg	90	114.618(2)	90.1244(15)	90	90
γ, deg	90	105.162(2)	90	90	90
V, Å^3	1702.22(15)	4218.4(4)	3391.77(18)	3688.3(2)	1671.05(15)
Z	4	4	4	4	4
cryst syst	Orthorhombic	Triclinic	Monoclinic	Orthorhombic	Orthorhombic
space group	P 2$_1$ 2$_1$ 2	P -1	P 1 21/n 1	P 2$_1$ 2$_1$ 2$_1$	P 2$_1$ 2$_1$ 2
d$_{calcd}$, g/cm^3	1.645	1.628	1.657	1.627	1.486
θ range, deg	1.832 to 30.581	1.289 to 26.372	1.822 to 36.252	2.035 to 36.442	2.342 to 30.569
μ, mm^{-1}	1.595	1.367	1.662	1.482	1.675
abs cor	Semi-empirical from equivalents	Semi-empirical from equivalents	Semi-empirical from equivalents	Semi-empirical from equivalents	Semi-empirical from equivalents
GOF^c	1.172	1.077	1.175	1.070	1.082
R1,^{a} wR2^b (I > 2σ(I))	0.0142, 0.0352	0.0264, 0.0669	0.0378, 0.0791	0.0325, 0.0638	0.0342, 0.0898

^{a} R1 = Σ | |F$_o$|-|F$_c$| | / Σ|F$_o$| ^{b} wR2 = { Σ [w(F$_o^2$-F$_c^2$)^2] / Σ [w(F$_o^2$)^2] }$^{1/2}$ ^{c} GOF = S = { Σ [w(F$_o^2$-F$_c^2$)^2] / (n-p) }$^{1/2}$

EPR Details

Spectrum was collected on an X-band EPR (Frequency: 9.391 GHz; Power: 0.645 mW; Modulation Amplitude: 1 G) as a toluene glass at 77 K. EPR simulation run using EasySpin program for Matlab.[17] Simulation parameters: g = [2.128, 2.032, 1.930], lw = 2, HStrain = [20, 20, 20], Nucs = 'Co', A = [119 65 105].
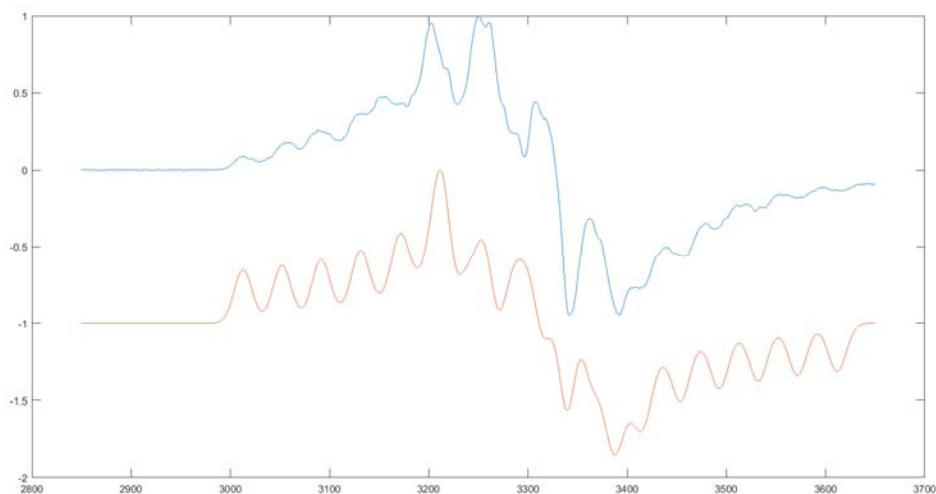
Figure S35. X-band EPR spectrum of **3** collected at 77K in a toluene glass (blue). EasySpin simulation of EPR data (red).

References

1.   Pangborn, A. B.; Giardello, M. A.; Grubbs, R. H.; Rosen, R. K.; Timmers, F. J., Safe and convenient procedure for solvent purification. *Organometallics* **1996,** *15* (5), 1518-1520.
2.   Zhao, Y. L.; Liu, L. H.; Zhang, W. Y.; Sue, C. H.; Li, Q. W.; Miljanic, O. S.; Yaghi, O. M.; Stoddart, J. F., Rigid-Strut-Containing Crown Ethers and [2]Catenanes for Incorporation into Metal-Organic Frameworks. *Chem. Eur. J.* **2009,** *15* (48), 13356-13380.
3.   Velian, A.; Lin, S. B.; Miller, A. J. M.; Day, M. W.; Agapie, T., Synthesis and C-C Coupling Reactivity of a Dinuclear Ni-I-Ni-I Complex Supported by a Terphenyl Diphosphine. *J. Am. Chem. Soc.* **2010,** *132* (18), 6296-6297.
4.   Murahashi, T.; Nagai, T.; Okuno, T.; Matsutani, T.; Kurosawa, H., Synthesis and ligand substitution reactions of a homoleptic acetonitrile dipalladium(I) complex. *Chem. Commun.* **2000,** (17), 1689-1690.
5.   Edgell, W. F.; Lyford, J., Preparation of Sodium Cobalt Tetracarbonyl. *Inorg. Chem.* **1970,** *9* (8), 1932-1933.
6.   Strong, H.; Krusic, P. J.; San Filippo, J., *Inorganic Syntheses.* 1986; Vol. 24.
7.   Fulmer, G. R.; Miller, A. J. M.; Sherden, N. H.; Gottlieb, H. E.; Nudelman, A.; Stoltz, B. M.; Bercaw, J. E.; Goldberg, K. I., NMR Chemical Shifts of Trace Impurities: Common Laboratory Solvents, Organics, and Gases in Deuterated Solvents Relevant to the Organometallic Chemist. *Organometallics* **2010,** *29* (9), 2176-2179.
8.   1)   Gaussian 09, Revision C.01, Frisch, M. J.; Trucks, G. W.; Schlegel, H. B.; Scuseria, G. E.; Robb, M. A.; Cheeseman, J. R.; Scalmani, G.; Barone, V.; Mennucci, B.; Petersson, G. A.; Nakatsuji, H.; Caricato, M.; Li, X.; Hratchian, H. P.; Izmaylov, A. F.;

Bloino, J.; Zheng, G.; Sonnenberg, J. L.; Hada, M.; Ehara, M.; Toyota, K.; Fukuda, R.; Hasegawa, J.; Ishida, M.; Nakajima, T.; Honda, Y.; Kitao, O.; Nakai, H.; Vreven, T.; Montgomery, Jr., J. A.; Peralta, J. E.; Ogliaro, F.; Bearpark, M.; Heyd, J. J.; Brothers, E.; Kudin, K. N.; Staroverov, V. N.; Kobayashi, R.; Normand, J.; Raghavachari, K.; Rendell, A.; Burant, J. C.; Iyengar, S. S.; Tomasi, J.; Cossi, M.; Rega, N.; Millam, J. M.; Klene, M.; Knox, J. E.; Cross, J. B.; Bakken, V.; Adamo, C.; Jaramillo, J.; Gomperts, R.; Stratmann, R. E.; Yazyev, O.; Austin, A. J.; Cammi, R.; Pomelli, C.; Ochterski, J. W.; Martin, R. L.; Morokuma, K.; Zakrzewski, V. G.; Voth, G. A.; Salvador, P.; Dannenberg, J. J.; Dapprich, S.; Daniels, A. D.; Farkas, Ö.; Foresman, J. B.; Ortiz, J. V.; Cioslowski, J.; Fox, D. J. Gaussian, Inc., Wallingford CT, 2009.

9.   (a) Tao, J. M.; Perdew, J. P.; Staroverov, V. N.; Scuseria, G. E., Climbing the density functional ladder: Nonempirical meta-generalized gradient approximation designed for molecules and solids. *Phys. Rev. Lett.* **2003,** *91* (14); (b) Staroverov, V. N.; Scuseria, G. E.; Tao, J. M.; Perdew, J. P., Comparative assessment of a new nonempirical density functional: Molecules and hydrogen-bonded complexes. *J. Chem. Phys.* **2003,** *119* (23), 12129-12137.

10.   (a) Jensen, K. P., Bioinorganic Chemistry Modeled with the TPSSh Density Functional. *Inorg. Chem.* **2008,** *47* (22), 10357-10365; (b) Buhl, M.; Kabrede, H., Geometries of transition-metal complexes from density-functional theory. *J. Chem. Theory Comput.* **2006,** *2* (5), 1282-1290; (c) Waller, M. P.; Braun, H.; Hojdis, N.; Buhl, M., Geometries of second-row transition-metal complexes from density-functional theory. *J. Chem. Theory Comput.* **2007,** *3* (6), 2234-2242.

11.   Hay, P. J.; Wadt, W. R., Abinitio Effective Core Potentials for Molecular Calculations - Potentials for the Transition-Metal Atoms Sc to Hg. *J. Chem. Phys.* **1985,** *82* (1), 270-283.

12.   Ditchfield, R.; Hehre, W. J.; Pople, J. A., Self-Consistent Molecular-Orbital Methods .9. Extended Gaussian-Type Basis for Molecular-Orbital Studies of Organic Molecules. *J. Chem. Phys.* **1971,** *54* (2), 724-728.

13.   Neese, F., *Wiley Interdiscip. Rev.: Comput. Mol. Sci.*, **2012**, *2*, 73-78.

14.   NBO 6.0. Glendening, E. D., Badenhoop, J. K., Reed, A. E., Carpenter, J. E., Bohmann, J. A., Morales, C. M., Landis, C. R., Weinhold, F. (Theoretical Chemistry Institute, University of Wisconsin, Madison, WI, 2013), http://nbo6.chem.wisc.edu/

15.   APEX2, Version 2 User Manual, M86-E01078, Bruker Analytical X-ray Systems, Madison, WI, June 2006.

16.   Sheldrick, G. M. "SADABS (Version 2008/1): Program for Absorption Correction for Data from Area Detector Frames", University of Göttingen, 2008.

17.   Stoll, S.; Schweiger, A., EasySpin, a comprehensive software package for spectral simulation and analysis in EPR. *J. Magn. Reson.* **2006,** *178* (1), 42-55.